CHARACTERIZATION OF LIVER X RECEPTOR- AND RETINOID ACID RECEPTOR-MEDIATED RESPONSE WITH TRANSCRIPTOMIC AND HISTOLOGICAL ANALYSIS IN ZEBRAFISH LIVER

HENDRIAN SUKARDI
B.Sc. (Honors), U of T

A THESIS SUBMITTED FOR THE DEGREE OF MASTER OF SCIENCE

DEPARTMENT OF BIOLOGICAL SCIENCES

NATIONAL UNIVERSITY OF SINGAPORE
2010

CHARACTERIZATION OF LIVER X RECEPTOR- AND RETINOID ACID RECEPTOR-MEDIATED RESPONSE WITH TRANSCRIPTOME AND HISTOLOGICAL ANALYSIS IN ZEBRAFISH LIVER

HENDRIAN SUKARDI

NATIONAL UNIVERSITY OF SINGAPORE
2010

Acknowledgements

I would like to thank to my supervisors, Professor Gong Zhiyuan and Dr. Lam Siew Hong, who have been supportive and helpful in providing me guidance throughout my graduate studies. Professor Gong offered me a valuable opportunity to do graduate study in his lab. Dr Lam Siew Hong provided me a lot of guidance and training to be a critical thinker and a good scientist.

I would like to give special thanks to Myintzu Hlaing, Zhan Huiqing and Svitlana Korzh whom I have bothered a lot and have provided me lots of assistance and guidance on benchwork. I learnt a lot of benchwork skills from them and they helped me in some of my experiments, and I would probably not been able to accomplish much lab results without them.

I also would like to thank my labmates who also helped me in my experiments and making the lab a nice place to be in: Grace, Li Zhen, Xu Dan, Preethi, Hongyan, Li Yan, Balang, Choong Yong, Yin Ao, Caixia, Grace, Tina, Weiling, Zhou Li, Lili and other labmates.

In addition, I would like to thank my family and friends for supporting me throughout the research. I would also like to give special thanks to Albert Goedbloed, Hendrick Sukardi, Henry Sukardi (Butok), Zhan Huiqing, Nicholas Karl Romanidis and Yevgeniy Igorovich Nikitin (Jenya) for providing moral and emotional support when I greatly needed them throughout my studies. People come and go, but real good friends remain together.

I dedicate this thesis to my former, but special, biochemistry teacher, Professor Emeritus Robert Kincaid Murray.

To Monty python group, who never cease to make me wonder whether a swallow can carry a coconut? If it can, is it an African or European swallow?

Table of Contents

Results and Discussion

Summary

Nuclear receptor, a class of ligand-activated transcription factor, regulates many important physiological processes. Therefore nuclear receptors, such as liver x receptor (LXR) and retinoic acid receptor (RAR), are attractive therapeutic targets. Although the zebrafish is a prominent vertebrate model that has recently gained surging interest for disease modeling and drug screening, currently little is known with regards to LXR- and RAR-induced responses in zebrafish liver. In our efforts to investigate the potential of zebrafish as a model for LXR- and RAR-related studies, we performed experiments using adult male zebrafish exposed to all-trans retinoic acid (RAR agonist) or T0901317 (LXR agonist) for 96 hours before sampling the liver for histological, transcriptomic and real-time PCR analyses. We observed LXR and RAR activation modulate several biological processes involved in immune system and metabolic processes. Our transcriptomic analysis corroborated with our histological analysis and real-time PCR analysis. We were able to capture known effects of LXR and RAR activation as reported in mammalian models, suggesting conserved mode-of-actions between mammals and fish. Our findings indicate that zebrafish is a valid model for investigating LXR and RAR drug targets, LXR- and RAR-mediated disruptions and metabolic disorders.

List of Tables

List of Figures

List of Abbreviation

22R-HC	22-R-hydroxycholesterol
acads	acyl-Coenzyme A dehydrogenase, short chain
aco2	aconitase 2, mitochondrial
acta2	actin, alpha 2, smooth muscle, aorta
ACTB	beta-actin
Anti-DIG	anti-digoxigenin antibody
arg2	arginase, type II
Arp	actin related protein
arpc1a	actin related protein 2/3 complex, subunit 1A
atp5h	ATP synthase, H+ transporting, mitochondrial F0 complex, subunit d
ATRA	All-trans retinoic acid
BCIP	5-Bromo-4-chloro-3-indolyl phosphate
BCR	B cell antigen receptor
BPA	bisphenol
c8a	complement component 8, alpha polypeptide
c9	complement component 9
casp7	caspase 7
casp8	caspase 8
cox10	heme A: farnesyltransferase (yeast)
cryabb	crystallin, alpha B, b
cyp26a1	cytochrome P450, family 26, subfamily a, polypeptide 1
dlst	dihydrolipoamide S-succinyltransferase (E2 component of 2-oxo-glutarate complex)

dlst	dihydrolipoyllysine-residue succinyltransferase component of 2-oxoglutarate dehydrogenase complex, mitochondrial
f10	coagulation factor X
fasn-like	fatty acid synthase-like
FDR	false discovery rate
fos	V-fos FBJ murine osteosarcoma viral oncogene homolog
g6pca	glucose-6-phosphatase a, catalytic
gclc	glutamate-cysteine ligase catalytic subunit
GSEA	Gene Set Enrichment Analyses
H&E	hematoxylin and eosin
HDAC	histone deacetylase
Hh	Hedgehog
hnf1ba	HNF1 homeobox Ba
IACUC	Institutional Animal Care and Use Committee
igf1	insulin-like growth factor 1
IL-2	interleukin-2
ins	insulin
itga9	integrin, alpha 9 homolog
jun	V-jun sarcoma virus 17 oncogene homolog (avian)
LMH	Low, Mid and High
LOC563884	transforming growth factor beta 1-like
LXR	liver X receptor
mlh1	mutL homolog 1, colon cancer, nonpolyposis type 2 (E. coli)

mmp9	matrix metallopeptidase 9
MMPs	Matrix Metalloproteinases
MODY	Maturity onset Diabetes of the Young
MSigDB	Molecular Signatures Database
NBT	Nitroblue tetrazolium
ndrg1	myc downstream regulated gene 1
NES	normalized enrichment scores
NRF2	Nuclear factor erythroid 2-like factor 2
OST	olfactory signal transduction
plg	plasminogen
pros1	protein S (alpha) homolog
psma3	proteasome (prosome, macropain) subunit, alpha type, 3
RAR	retinoic acid receptor
rel	reticuloendotheliosis viral oncogene homolog
ROS	reactive oxygen species
rpl13a	60S ribosomal protein L13a
slc25a27	protein kinase, solute carrier family 25, member 27
SMRT	silencing mediator of retinoic acid and thyroid hormone receptor
	spp1 homolog secreted phosphoprotein 1 homolog
TCA	Tricarboxylic acid
TF	tissue factor
TGF- ß	Transforming growth factor ß
vcam1	vascular cell adhesion molecule 1

VPA	valproic acid

Chapter 1
Introduction

1.1 Zebrafish as an attractive model for vertebrate development studies

The zebrafish (*Danio rerio*) is a small freshwater tropical fish that is endemic to northern India. Since early 1970s, George Streisinger and his colleagues have characterized the use of zebrafish as a model organism for embryogenesis (Sreisinger et al., 1981; Detrich et al., 1999), and it has recently become a popular model organism for studying vertebrate development and gene function. They complement higher experimental vertebrate models, such as rats and mice, due to its numerous innate advantages. First, female zebrafish produce large clutches (100-200) of embryos per week. Secondly, the zebrafish has fast embryonic development, whereby cleavage divisions, gastrulation, morphogenesis, and organogenesis occur within 24 hours, and zebrafish embryos develop into larvae in less than three days. Thirdly, the embryos are large, transparent and develop externally to the mother. Thus taken all above, these attributes greatly facilitates experimental observation and manipulation using zebrafish.

1.2 Zebrafish as an emerging model for toxicology and chemical biology using omics

The zebrafish is an attractive lower vertebrate model for energy metabolism (Schlegel and Stainier, 2007) and immune studies (Sullivan and Kim, 2008), since it shares many similar important physiological attributes with mammals (Schlegel and Stainier, 2007). The zebrafish has long been used as an experimental model to study chemical toxicity

ranging from mutagens, carcinogens, teratogens to direct toxicants since 1950s (Laale, 1977). From 1980s to mid-90s the zebrafish became a premier vertebrate developmental and genetic model, and within the next decade it has positioned itself as a biomedical model for various human disorders that could aid in discovering novel therapeutics. Several recent studies, including ours, have shown conserved chemical-induced organ/tissue responses between zebrafish and humans (Parng et al., 2002; Peterson et al., 2004; Hill et al., 2005; Lam et al., 2006; Lieschke and Currie, 2007; Lam et al., 2008; Tilton et al., 2008; Webb et al., 2009). Furthermore, there are recent surging interests in using zebrafish for disease modeling, drug-induced perturbations and drug screening (Stern and Zon, 2003; Zon and Peterson, 2005). Moreover, the zebrafish is small, available in large numbers and maintained at lower husbandry cost than rodents. Thus zebrafish can complement as a more cost-effective model to rodent in drug characterization studies.

The zebrafish is amenable to various molecular techniques, and a large and increasing number of mutant and transgenic lines available for modeling human diseases have added further value to the system. Recently, the availability of vast genomic resources in zebrafish and the ability to map zebrafish genes to mammalian homologs make it feasible to apply omics approaches to chemical biology for identifying molecular biomarkers and providing mechanistic insights into biological responses during chemical perturbation and subsequently potential health-risk inferences to humans (Parng et al., 2002; Peterson et al., 2004; Hill et al., 2005; Lieschke and Currie, 2007).

Omics approaches involve high-throughput technologies that allow characterization of chemical-induced perturbations from the measurement of global changes in the abundance of mRNA transcripts (transcriptome), proteins (proteome), and other biomolecular components (metabolome) in complex biological systems. They have revolutionized research in drug development and toxicology (Butcher et al., 2004; Harrill and Rusyn, 2008; Blomme et al., 2009). By capturing the global profile of the biological responses, investigation into the mode of action and toxicity of a chemical can be facilitated. Furthermore, an omics database of chemicals can establish to help predict pharmacological efficacy and toxicological effects of a new chemical and to improve the selection of drug candidate (Ganter et al., 2005).

1.2.1 Mechanistic omics

With appropriate experimental design, omics data can provide mechanistic information about the mode of action and toxicity of a chemical via knowledge-based data mining to identify pathways and biological processes associated with the chemical perturbation. By coupling traditional phenotypic endpoints with omics data, the mechanism of chemical action and toxicity can be defined in a conceptual framework of cause-and-effect with supports from known molecular interactions and phenotypic anchoring (Paules, 2003). In one early study in rats, mechanistic action of estrogen induction of uterine growth and maturation has been defined by linking differentially expressed gene sets and associated biological processes to physiological and morphological changes in uterine during its growth (Moggs et al., 2004). This study has anchored the phenotypic changes in uterine

and revealed that uterine growth and maturation are preceded and accompanied by a complex molecular program, beginning with the induction of genes involved in transcriptional regulation and signal transduction and followed sequentially by genes in protein biosynthesis, cell proliferation, and epithelial cell differentiation. Thus, this study has provided a mechanistic view of the estrogen-induced transcriptional program that modulates the uterotropic responses.

Using a similar approach, several transcriptomic profiling studies have yielded novel mechanistic insights into the mode of action and toxicity of several chemicals in zebrafish. In one study, the mechanism of teratogenic action of valproic acid (VPA) has been determined by comparing the effects of known histone deacetylase (HDAC) inhibitors and noninhibitory VPA analogs in zebrafish embryos (Gurvich et al., 2005). These tetratogens induce similar tetratogenic effects that are characterized by pericardial effusion, crooked tails, abnormal gut coiling, reduced pigmentation, and defective eyes. Transcriptomic analysis has revealed that the effects of VPA and trichostatin A, a structurally unrelated HDAC inhibitor, are highly concordant. Together with phenotypic assays, the study has further demonstrated that inhibition of HDACs is likely the mechanism leading to the teratogenic effects of VPA.

In another study, cyclopamine, an inhibitor of Hedgehog (Hh) signaling, has been used to identify Hh-regulated genes (Xu et al., 2006). By comparing transcriptome profiles of wild-type zebrafish embryos, cyclopamine-treated embryos, and Hh-enhanced embryos by injection of RNA coding for dominant negative version of protein kinase A, a large set

of Hh signaling responsive genes enriched with Gli-binding motif has been identified and further validated by reverse transcription (RT)-polymerase chain reaction and phenotype-based in situ hybridization (Xu et al., 2006). The Hh signaling responsive genes discovered in this study are useful for elucidating the mechanism of Hh signaling not only in normal development but also in aberrant signaling to model human diseases.

In a study investigating genes that mediate addiction to amphetamine, the adult brain transcriptomes of wild-type zebrafish and mutant no addition ($nad^{dne3256}$), which is unresponsive to amphetamine, in the presence and absence of amphetamine have been compared, and a new network of coordinated gene regulation associated with amphetamine-triggered addictive behavior has been revealed (Webb et al., 2009). Interestingly, the differentially expressed gene set is significantly enriched with transcription factor genes that are also involved in vertebrate brain development. Further phenotypic analysis with in situ hybridization has shown that these genes are also active in adult brains. Thus, these amphetamine-modulated genes are involved in neuro-development and subsequently mediate behavioral addiction to amphetamine. These transcriptomic studies have demonstrated the use of chemical or genetic modifiers to generate loss- or gain-of-function phenotypes in zebrafish to yield valuable mechanistic insights.

Transcriptomic data have also been used to investigate mechanism of toxicity of chemicals. For example, the mechanistic action of copper-induced olfactory injury in zebrafish has been analyzed with transcriptome profiling (Tilton et al., 2008).

Differentially expressed genes are enriched with components of a highly conserved olfactory signal transduction (OST) pathway involving genes for calcium transport and channel, olfactory receptors, divalent ions, ion channels, and G-proteins. Interestingly, these genes in the OST pathways are repressed, suggesting that they become insensitive to odorants due to copper-induced injury. Thus, this study has demonstrated that the zebrafish olfactory system is a feasible model to perform diagnostic study of how different chemicals affect the conserved OST pathway. In another study, mechanism of toxicity of a polybrominateddiphenyl ether, 6-hydroxy-BDE47, commonly used as a flame retardant, has been investigated via transcriptomic profiling of zebrafish embryonic fibroblasts under exposed and unexposed conditions (van Boxtel et al., 2008). Gene-ontology-based analysis has revealed that genes involved in proton transport and carbohydrate metabolism are enriched; therefore suggesting that oxidative phosphorylation is disrupted. The uncoupling of oxidative phosphorylation has been confirmed by in vitro biochemical assay of zebrafish mitochondria. Hence, this study raises questions on the impact of polybrominateddiphenyl ethers in the environment, including health-risk posed to humans and other organisms. In our ongoing study for mechanistic insight and health-risk effect of early life exposure to BPA, a chemical used in the manufacture of polycarbonate plastic that has caused wide concern due to its high exposure in humans and potential health effects, transcriptome profiles of BPA-treated and control zebrafish embryos have been examined. We can identify deregulated signaling pathways such as ephrin receptor, clathrin-mediated endocytosis, synaptic long-term potentiation, and axonal guidance that are associated with neurological development, function, and pathology. The effect has been further validated using a

transgenic zebrafish line, Tg(nkx2.2a:mEGFP), that fluoresces green in the central nervous system (Ng et al., 2005). The findings in zebrafish are in agreement with the main health concerns of early-life exposure to BPA in humans with regard to its impact on the nervous system (Chapin et al., 2008). These studies have further demonstrated how mechanistic insights obtained from transcriptome analyses can be validated through other independent assays amenable in the zebrafish system.

1.2.2 Comparative omics application with repository databank

Gene signatures defined from transcriptomic profiling can be used for generation of novel associations and insights among different biological states perturbed by chemical compounds, biomolecules, and diseases within the same species and across different species. Comparison of omics signatures provides an in silico approach for determining chemical action and toxicity, as well as for identifying chemicals that may cause or treat a disease. Omics database repositories offer ample opportunities for various comparative and meta-analyses to gain novel insights. For example, by comparing their gene signatures with other signatures of chemicals with known mechanistic action in Connectivity Map database (www.broadinstitute.org/cmap/) (Lamb et al., 2006), it has been discovered that both celastrol and gedunin, which are structurally similar natural products for medicinal and anticancer use, have yet unknown inhibitory role for HSP90 activity (Hieronymous et al., 2006). This study illustrates the power of comparative chemical genomics for discovery of new roles of chemicals as well as their novel mechanistic insights.

Recently, we have also found via the same comparative approach that mercury-induced hepatotoxicity in zebrafish has similar responses as the mercury-treated human liver cell line, HepG2 (GEO Accession GSE6907) (Ung et al., 2010). Several significantly enriched canonical pathways are deregulated in both systems. DNA damage signaling and proteasome pathway are up-regulated, whereas pathways of nuclear receptor signaling, mitochondrial fatty acid beta-oxidation, and electron transport chain are down-regulated. Moreover, we have also captured additional deregulated metabolic processes such as fatty acid synthesis and gluconeogenesis in zebrafish livers but not in the human HepG2 cells, indicating the importance of in vivo modeling to provide the whole-organism context and physiology for capturing certain pathway at organ and system levels.

1.2.3 Transcriptomic approaches in chemical perturbation studies in zebrafish

Several of these chemical perturbation studies using omics approaches have made relevant associations and inferences to human health-risks. In addition, omics profiling of normal physiological state and various developmental stages of zebrafish have been performed and these can serve as reference data for comparative analysis in future chemical studies.

1.2.4 Transcriptomics

Transcriptomics involves the measurement of global changes in the abundance of different mRNA species in a biological sample. It generates inferences to transcription of genes and potentially translation of gene products and thereby provides a molecular perspective of a biological state. The current transcriptome profiling tools used in zebrafish are microarray and RNA-Seq. Microarray is a closed platform with predefined gene probes spotted onto a solid support, which is then hybridized with fluorescent-labeled cDNA prepared from RNA samples. The abundance of an mRNA species is estimated based on the relative fluorescent intensity on each probe. RNA-seq, or deep sequencing of RNA samples using the next generation of sequencing technology, is recently becoming a popular transcriptome profiling tool as it is an open platform because it does not require predefined probes. In principle, RNA-seq profiles all transcripts, including novel ones that have not been previously characterized. In general, RNA-seq yields data with higher resolution, wider dynamic range, and lower background noise, and it requires lesser amount of RNA sample than microarrays (Wang et al., 2009; Wilhelm and Landry, 2009). Although there is currently no published literature in RNA-seq on chemical perturbation in zebrafish, it has been used to profile transcriptome response to mycobacterium infection in adult zebrafish (Hegedus et al., 2009). The results of differentially expressed genes obtained with RNA-seq are concordant with the previous data based on microarrays (Meijer et al., 2005).

As for microarray platforms, two large-scale proof-of-principle studies involving multiple (>10) chemicals have been reported for zebrafish toxicology and chemical biology (Yang et al., 2007; Lam et al., 2008). Microarray has been shown to be a sensitive tool for capturing chemical-induced tissue-specific responses in zebrafish embryos (Yang et al., 2007). This has been validated with in situ hybridization assays by showing that the responsive genes are highly restricted to specific organs or cells. Moreover, chemical-specific GE profiles with predictive power can be obtained using zebrafish embryos. Similarly, our group has performed such studies using adult zebrafish and found that whole-adult zebrafish chemogenomics is also useful for predictive and discovery chemical biology (Lam et al., 2008). We have generated robust prediction models and yielded information on biomarkers of effects and deregulated signaling pathways. These are important not only for developing a molecular tool for predicting chemical exposure but also for understanding perturbed biological functions and physiological systems and thus for inferring health-risks to human.

In one study, disruptive effects of antidepressant mianserin on estrogenic signaling in zebrafish brain and gonadal have been analyzed (van der Ven et al., 2006). The transcriptome profiling data suggest that the estrogenic effect is caused by perturbation in hypothalamo-pituitary-gonadal axis by mianserin-induced deregulation of serotonergic and adrenergic systems in the brain. In another report on system-wide responses of the hypothalamo-pituitary-gonadal axis in zebrafish to endocrine-active chemicals, transcriptome profiles of brain and ovarian tissues of zebrafish treated with aromatase inhibitor fadrozole have been analyzed (Villeneuve et al., 2009). Fadrozole induces

neurodegenerative stress in the brain tissue, and radial glial cells are proliferated to cope with the stress. In the ovary of fadrozole-treated zebrafish, disruption of oocyte maturation and ovulation is caused by impaired vitellogenesis. These two studies (van der Ven et al., 2006; Villeneuve et al., 2009) illustrate that transcriptomic profiling could capture the mechanistic actions of anti-depressants in brain and reproductive tissues in zebrafish and the effects may be inferred to humans.

In a study that investigated molecular mechanism of toxicity and carcinogenicity of arsenic, we have performed microarray analysis on liver of zebrafish exposed to arsenic for 8–96h to identify deregulated biological networks (Lam et al., 2006). Many of the differentially expressed genes identified are involved in heat-shock response, DNA damage/repair, antioxidant activity, hypoxia induction, iron homeostasis, arsenic metabolism, and ubiquitin-dependent protein degradation. These suggest strongly that DNA and protein damage as a result of arsenic metabolism and oxidative stress caused major cellular injury. These findings are comparable with those reported in mammalian systems, hence highlighting the potential of zebrafish for health-risk inferences. Another study has shown that two of the biomarker genes for prenatal arsenic exposure in humans, foxo5 (zebrafish ortholog of human FOXO3A) and pik3r1, have also been captured in transcriptomic profiles of arsenic-treated zebrafish embryos (Mattingly et al., 2009). Therefore, most zebrafish transcriptomic studies involving chemical perturbation mainly focused on investigating molecular mechanism and effects, or to identify biomarker/target genes as well as for comparative analyses.

1.3 Nuclear Receptors

Nuclear receptors are a class of transcription factor proteins which are present in the interior cells and detect the presence of steroid, hormones and other molecules. These receptors work in concert with other proteins to modulate various biological processes such as development, homeostasis and metabolism of the organism via regulating transcription of specific genes. The nuclear receptor-mediated regulation of gene expression occurs when a ligand is present. The ligand binding to a nuclear receptor results in conformational change and subsequently activates the receptor. Therefore, the activated receptor has ability to directly bind to targeted segments of genomic DNA and thus modulates targeted gene transcription.

Since nuclear receptors regulate many biological processes and are directly activated with ligands, they are attractive novel targets for drug therapy (Tobin and Freedman, 2006) and there are also interests in their associations with endocrine disruptive environmental pollutants by deregulating nuclear receptor signaling (Grum and Blumberg, 2006). There are also interests in using zebrafish in developmental screens to identify ligands of selected nuclear receptor for drug screens and endocrine disruptors (Tiefenbach et al., 2010). In this study, we characterized nuclear receptor-activated biological responses by two receptors: liver X receptor (LXR) and retinoic acid receptor (RAR). Information generated in this study can facilitate future studies in drug screening and also help characterize LXR and RAR disruptors.

1.3.1 Liver X receptor

LXRs are oxysterol-activated transcription factor and their ligands include natural oxysterols 22-R-hydroxycholesterol (22R-HC), 24,25(S)-epoxycholesterol, and 27-hydroxycholesterol, and synthetic compounds T0901317 and GW3965 (Collins et al., 2002; Russell, 1999). Activated LXRs form heterodimers with retinoid X receptor and regulate gene transcription via binding to LXR response elements in the promoter regions of target genes (Repa et al., 2000). In mammals, there are two LXR isoforms, LXRα (NR1H3) and LXRβ (NR1H2). While mammalian LXRβ are ubiquitously expressed, mammalian LXRα are highly expressed in the liver and at lower levels in macrophages, adipose tissue, kidney, lung, adrenal glands and intestine (Maglich et al., 2003). Zebrafish and fugu contain only one single LXR gene which has higher similarity in gene sequence with mammalian LXRα (Archer et al., 2008; Maglich et al., 2003). However zebrafish and fugu LXR, like mammalian LXRβ, are ubiquitously expressed in all examined tissues (Archer et al., 2008; Maglich et al., 2003). Zebrafish LXR has been shown to be activated by 22R-HC, GW3965 and T0901317 based on induction of several known LXR transcriptional target genes (Archer et al., 2008).

LXR regulates glucose and lipid metabolisms, and also modulates immune and inflammatory responses (Baranowski, 2008; Joseph et al., 2003; Zelcer and Totonoz, 2006), hence it is a potential therapeutic target for atherosclerosis, diabetes and rheumatoid arthritis (Cao et al. 2003; Chintalacharuvu et al., 2007; Joseph et al., 2002; Li et al., 2010a; Repa and Mangelsdorf, 2002). For example, T0901317 has been shown to

reduce glucose levels and improve insulin sensitivity in rodent models for diabetes (Cao et al., 2003), highlighting the potency and feasibility of LXR as a drug target. However, LXR activation is also associated with adverse effects such as hepatic steatosis and hypertriglyceridemia in mice (Baranowski, 2008). Furthermore administration of T0901317 induced more severe hepatic lipogenesis in diabetic mouse models than the non-diabetics (Chisholm et al., 2003). The lipogenic effects of T0901317 leads to an increase of triglyceride and non-high density lipoprotein cholesterol in hamsters and monkeys in preclinical studies and thus outweighs the desired beneficial effects (Li et al., 2010b). Therefore these adverse effects have impaired the advancement of T0901317 into clinical trials (Li et al., 2010b).

We have previously shown that chemical agonists that activate two other nuclear receptors (aryl hydrocarbon receptor and estrogen receptor) induced highly-conserved responses in zebrafish that can be inferred to humans (Lam et al., 2008). As to LXR, although its tissue distribution and developmental expression patterns had been characterized in zebrafish (Archer et al., 2008), little is known with regard to LXR-induced transcriptomic responses in zebrafish liver.

1.3.2 Retinoic acid receptor

RAR is a nuclear receptor that is activated by retinoic acids (9-cis retinoic acid and all-trans retinoic acid) (Kane et al., 2008; Tang and Russell, 1990). There are three RAR orthologs in mammals: RAR-α, RAR-β and RAR-γ. In zebrafish, there are RAR-α a, α b,

γ a and γ b (Hale et al., 2006; Waxman and Yelon, 2007). Retinoic acids, oxidized forms of vitamin A, bind to RAR and result in activation of RAR. Subsequently, they modulate development, immune function, lipid metabolism, differentiation and proliferation (Lefebvre et al., 2005; Stephensen, 2005). Retinoid acids are also widely used in dermatological and cancer treatments (Lefebvre et al., 2005). All-trans retinoic acid (ATRA) is the most abundant retinoic acid isomer in vivo and the most well-characterized RAR agonist (Kane et al., 2008; Tang and Russel, 1990), hence it is selected for our treatment.

Most of the retinoic acids in humans are obtained thru ingestion of vitamin A which is derived from animal food products (such as liver), multivitamin supplements and fortified foods (Allen and Haskell, 2002). Observational studies suggest that more than 75% of the population in developed nations may consume vitamin A regularly more than the recommended dietary allowance (Allen and Haskell, 2002). Most experimental studies have characterized the benefits of vitamin A supplements and adverse effects of vitamin A deficiency, but there are little studies on toxic effects of excessive vitamin A (hypervitaminosis A), especially at subtoxic levels (Penniston and Tanumihardjo, 2006).

1.4 Main objectives and significance of the study

Nuclear receptors regulate many important biological processes, thus this group is an attractive therapeutic drug target. The zebrafish is one of the most well-studied fish species and it is economical for evaluating potential health-risk of chemicals. There are

increasing interests to use zebrafish for disease modeling and drug screening. Thus characterization of the effects of nuclear receptors disruption on biological function can be studied in zebrafish.

Our lab has been studying system-wide and comprehensive biological effects of chemical perturbations using microarrays (Lam et al., 2008; Lam et al., 2006a; Ung et al., 2010). We have characterized effects of chemicals that activate nuclear receptors such as estrogen and aryl hydrocarbon receptors (Lam et al., 2008). In this study, we characterized biological effects induced by LXR and RAR in zebrafish liver with its respective agonist ligands, T0901317 and all-trans retinoic acid (ATRA). T0901317 and ATRA are potential therapeutic drugs (Lefebvre et al., 2005; Li et al., 2010b); however, they have adverse effect on metabolism by elevating triglyceride level (Cisneros et al., 2005; Li et al., 2010b). The liver is a major metabolic organ, hence drug-induced metabolic perturbations and hepatotoxicological effects can be studied in liver. We determined drug modulated molecular process at systems-wide level by both transcriptomic and histological analyses. The combination of molecular analysis with histological analysis, or phenotypic anchoring, allows construction of an in vivo mechanistic model of drug modulations in liver. Information in this study can also help future studies in drug screening directed at these nuclear receptors using zebrafish system.

Chapter 2
Materials and Methods

2.1 The zebrafish

Adult zebrafish (around 6 months old) were obtained from a local fish supplier. The fish were acclimatized for at least a week in aquaria before they were transferred into small tanks for T0901317 and all-trans retinoic acid (ATRA) exposure. For two types of experiments (i.e. histology and microarray), zebrafish were exposed to T0901317 and ATRA at different concentrations for 96 hours at density of 1 fish/200 mL at 27°C. For PCR gene validation, zebrafish were obtained from another subsequent treatment batch at a later date. Chemical solutions and water were changed daily. All experiments were performed in accordance to the guidelines of Institutional Animal Care and Use Committee (IACUC) and approved by IACUC.

2.2 T0901317 and all-trans retinoic acid treatment

T0901317 (chemical purity>98%, Sigma-Aldrich) and ATRA (chemical purity≥98%, Sigma-Aldrich) were chosen as liver x receptor (LXR) and retinoic acid receptor (RAR) agonists respectively. Both T0901317 and ATRA were dissolved in dimethyl sulfoxide (DMSO) as a vehicle solvent separately. Final DMSO concentration in all treatments and control was 0.05% (v/v). Treatment concentrations were chosen based on hepatic histopathological results produced from 96 hour treatment. Concentrations used for both treatments were 2000 nM, 200 nM and 20 nM. Microarray analyses of treatments were carried out in four to five replicate groups, each which had four pooled zebrafish livers.

2.3 Microarray experiments and transcriptome analysis with knowledge-based analysis

2.3.1 RNA extraction and DNA microarray experiments

Total RNAs from five replicates (each replicate consist of pooled livers from four fishes) after 96 hour treatment were isolated with Trizol reagent (Invitrogen, USA) protocol. Reference RNA was obtained by pooling total RNA from whole male and female wild-type zebrafish in 9:1 ratio.

We used two-color microarray experimental design to avoid labeling bias by Cy5 and Cy3 dyes; the reference RNA provides reference background (Cy3) signals that covers as many microarray gene probes as possible from male and female. The 9 male: 1 female ratio was found to be a suitable mixture of reference that avoids signal saturation from extreme highly-abundant transcripts that are specific in females such as vitellogenins. Therefore, this allows relatively good sensitive detection in the expression of female-specific genes in experimental samples from males by chemical treatments. If excessive female samples are used, the reference RNA could highly saturate probes for female-specific genes and thus the detection of the corresponding transcript signal in experimental samples will be masked. Conversely if none or inadequate female sample is used, the signal of reference on the corresponding probes will be absent or poor and thus over amplify signals of transcript from the experimental samples. We have found 9 male: 1 female reference ratio provided good reference signal that allows capture of changes in transcript abundance for our experimental data.

Reference RNA was co-hybridized with RNA samples either from control or treated fish on a poly-L-lysine-coated glass array spotted with 22 K zebrafish oligo probes. For fluorescence labeling of cDNAs, 10 μg of total RNA from the reference and sample RNAs were reverse transcribed and labeled differently, with fluorescent dyes Cy-3 and Cy-5, respectively. The microarray slides were hybridized at 42°C for 16 hours in hybridization chambers, then they were washed in a series of washing solutions (2x SSC with 0.1% SDS; 1x SSC with 0.1% SDS; 0.2x SSC and 0.05x SSC; 30 seconds each), dried with low-speed centrifugation and scanned for fluorescence detection with the GenePix 4000B scanner (Axon Instruments). Detailed protocols for microarray experiment and data acquisition can be further referred to our recent publications (Lam et al., 2009a, b).

2.3.2 Microarray data normalization and transcriptome analysis

Lowess method in the R package (http://www.braju.com/R/) was used to normalize the raw microarray data. Gene set enrichment analysis (GSEA) (Subramanian et al., 2005) was performed to characterize the molecular pathways or processes that are perturbed by T0901317 and ATRA. Another batch of fishes was retreated with T0901317 and ATRA, and quantitative real-time PCR was used to validate gene expressions that were significantly altered in relevant pathways or processes.

2.3.3 Transcriptome profile analysis with Gene Set Enrichment Analysis (GSEA)

Gene Set Enrichment Analyses (GSEA) was used to determine T0901317 and ATRA-modulated biological pathways as described in detail in (Subramanian et al., 2005). The zebrafish genes were mapped to human homologs as previously described in (Lam et al., 2006b). The human homologs of zebrafish genes from the transcriptome profiles were ranked according to the *p*-values with Student t-test. The "GSEAPreranked" option of GSEA was used. The ranking metric used was log10 (1/P) where P is the *p*-value of a gene from microarray data. Down-regulated genes have positive values of log10 (1/P) whereas up-regulated genes have negative values of log10 (1/P). The genes were later ranked in descending order based on values of log10 (1/P). The ranked list of genes for each concentration are compared to 1892 curated gene sets or signatures that are deposited in the Molecular Signatures Database (MSigDB) from the GSEA website. Statistical significance of the gene set for each concentration treatment was calculated using an empirical phenotype-based permutation test procedure. The number of permutation used was 1000. Pathways with false discovery rate (FDR) <0.25 were considered statistically significant, $0.25 \leq$ FDR <0.35 as marginally significant and FDR≥ 0.35 were not significant. Positive and negative values of normalized enrichment scores (NES) indicated up- and down-regulation of pathways, respectively. Further detailed protocols and principles used for GSEA scoring are described in methods section from our recent study (Ung et al., 2010).

2.3.4 Ingenuity Pathway Analysis

Network used to view connectivity of human homologs is generated with Ingenuity Pathways Knowledge Base software (www.ingenuity.com) from 58 leading edge genes in GSEA gene sets that are presented and were deregulated in LMH (Low, Mid and High) treatment group significantly (T-test $P<0.05$). Network scores are calculated based on the hypergeometric distribution and is calculated with the right-tailed Fischer's Exact Test.

2.4 Gene Validation with real time quantitative PCR

Quantification of gene expression level was performed on synthesized First Strand cDNA via quantitative Real-Time PCR reaction using LightCycler® 480 SYBR Green I Master kit according to manufacturer's protocol (Roche). Nine biological replicates in each concentration group were performed for all real-time PCR experiments. Quantification of transcript levels were measured by using relative quantification between PCR signal of the target transcript in treatment groups and untreated control group after normalization with the transcript level of 60S ribosomal protein L13a (*rpl13a*) for T0901317 treatment group and beta-actin (ACTB) for ATRA treatment group. The primers (Table 1 and 2) used in the study are listed below.

Table 1. Primers used for validating T0901317 treatment

Gene Symbol	Gene ID	Product length (bp)	Annealing Temperature (°C)	Sense primer	Antisense Primer
Lxr	BC092160	150	60	GAGATTCTCAGTCAAACGGACTTG	TGATGTCGTTGGATTCCATGA
fasn-like	BI880357	151	62	GGAGATGGATTGGGATCAGA	TGGGTTCAGACAGTGAGCTG
Fasn	AW077199	149	64	TGTAGACGCCAGTTTTGCTG	ATTTGACGCAGCCTTCTTTG
vcam1	AW344246	197	66	TCCTGCAGGGCGTATGGTGC	TCCTGGGAGGTGCTTTCACGGT
mmp9	AW174507	103	68	TGGACCAGCCATTCAAACCCGC	GCCCTCAGTGGTGCAGGTGG
itga9	BC054897	178	66	TGCCGGATCCGCAACAACCC	AGCGATGAGCGCAGGCCAAA
f10	BM154293	210	62	ATCGAGGAGGAACCAATCCT	ACAACCACCCTGATGGAGAG
pros1	BI887609	124	62	CTGCTGTCCGCTACACTCTG	CGCTCCAGGTTTCCTTTCT
Plg	BC059801	220	60	TCTGTAGTCCATGCCAATGC	CCTGCCAACTCAAAAACTGA
c8a	AW018673	166	68	TGCCTGCGGTCCAAAAGGACG	TCCCAGTGTGGCTTTGTCGGC
c9	AW019201	222	62	CGACCGATGAGTCAGATGAA	CCAACATTCCAGGGTAGTCG
Acads	BC079521	152	60	ATTAGCCAATCCAGGCAC	TGCGGAAAGACACTACAGAG
g6pca	BC076446	150	60	GCTCATTTCCCACACCAAGT	ATAAAAGCCCACAGCGAATG
igf1	AF268051	132	62	CGATCTCTACGAGCACAACG	TAGTTTCTGCCCCCTGTGTT
hnf1ba	AF430840	218	62	CGCTGTTTCCTCACATACCA	CGAGCAGAGGGCAGAAATAG
Ins	AF036326	200	64	AGTGTAAGCACTAACCCAGGCACA	TGCAAAGTCAGCCACCTCAGTTTC
rpl13a	BM153976	191	60	CATCTCCTCGGTCGTCTTTC	CTGGGGGCTCTGAAGTGATA

Table 2. Primers used for validating all-trans retinoic acid treatment

Gene Symbol	Gene ID	Product length (bp)	Annealing Temperature (°C)	Sense primer	Antisense Primer
cyp26a1	U68234	200	60	GAAAAGGCTTGAGCATGGAG	CCTCCGAAGGGGATGTAGTT
arpc1a	AI384833	159	58	CGCTTTCGTAACATGGACAA	TATGGTCATTGCTCCGTCAA
prkag1	BI885847	156	62	CCTGGACATCACCGTGACTA	ACAACCTCCTGCTCATCCAC
slc25a27	BC053139	138	60	GTCTTGTGTCTCCGCCTCTC	CACTGCTGCGAGTGTAGTGG
cox10	AW342801	237	62	CGTGCTGCTACACTCCTCTG	GATGGGTGACGGACATCATT
atp5h	CK400662	161	62	TGACTGTTCCTGAGCCTGTG	CTGATCGAAGGGGATCATGT
mlh1	AI558727	210	62	CTGGTCGTAAAACGCTCACA	GACTGTAGTGAACCGCATCG
Gclc	AW128066	163	60	CAAAACCTCCTTCCCATTCA	CGTAAGAAAACACGGCATCC
nfe2l2	CR848724	115	60	GGCGTTTACCCAGAATCCTT	ATCCAACGTCTCCTGCATTT
psma3	BG306038	241	62	GCTTGAAGCCTCTTCTCTGG	CGGAAGGGTATTTCAGGTTG
arg2	AW018735	165	62	TTAACGGCGGACTGACCTAC	CGGATGCAACTATGTCAACG
ndrg1	BM185420	209	60	TCATGGCTGAACAAGGTGTC	TCGAAACCTCTGATTGTGGA
casp7	BC095327	150	60	TGCCAATCCAAGACACAAGA	AGTTGCTTGCCGAACTCACT
casp8	AF273220	235	60	TCAAACGAACAGGCACTG	ACTTCTCGGATTTCAACTGG
aco2	BI888674	210	60	TCTTCTCTGACAGGGTGAGC	TGGCAACCTACTGCTTAACTG
Dlst	BI896563	246	60	CTGTGACAGACTCCGCAAAC	TGTGTCATTCCCGCTGTCT
Jun	BE605692	154	60	TTTTGCGACTTCAGGGTCTT	CACCGCTCTCTCCTATCGAC
Fos	BE605310	155	60	CAGCCCATGATCTCCTCTGT	CGGATTTTTCATCCTCAAGC
ppap2b homolog	BE201484	102	60	TATGGTGTCACCGCTTTGAG	TCAGTGCTCCAGCAGAAAGA
ppap2c homolog	AW115654	184	60	GCCTTTGCTGTGTATGTTGG	GCTCTTCGTTTACCGCATTC
tgfb1a	AW566567	181	62	AACGGAGACCTGCTGTATGC	ACCAGGGTTGTGGTGTTTGT
LOC563884	LOC563884	159	62	CATTGACTTCCGCAAAGACC	GCAGAGGCACCAGGATTATG
Cryabb	BC076518	186	60	TTGCACCAGAGGAGCTATCA	TCACTGTCAGCACACCATCA
spp1 homolog	CR925756	179	62	CGCTGTCTGTGCTTTCATTC	CCTCGTCGCCACAGTCTT
serpine1	BX470232	220	62	TCTCTGGCTGGCTGAAGTCT	CTAAAACTGCTCGCCTCCAA
acta2	CU855699	221	62	GCTCGATGGGGTACTTGAGA	GTGTGACGACGAAGAAAGCA
bactin2	AF025305	213	60	CATCACACCTTCTACAATGAGC	ATCACCAGAGTCCATCACG

2.5 Histological processing and analysis

2.5.1 Histological processing, sectioning, and hematoxylin and eosin staining

For the histological processing, adult zebrafish were treated with different concentrations (20 nM, 200 nM and 2000 nM) of T0901317 (>98%, Sigma-Aldrich) or ATRA (≥98%, Sigma-Aldrich) for 96 hours at a density of 1 fish/200 mL at 27 ± 2°C. The vehicle concentration of DMSO for the treatments is 0.05% (v/v) and control fish were kept in water with 0.05% (v/v) DMSO concentration. 6 fish were used in each group. Treatment and control solutions were changed daily. After treatment, the fishes were sacrificed. The digestive organs were exposed by slitting ventrally from heard to anus, and then 4 fish were fixed in Bouin's solution and remaining 2 fish are fixed in Formalin solution 10%, Neutral Buffered (Sigma-Aldrich), for 1 week at room temperature. The tissue samples were then washed several times with 70% ethanol, dehydrated in a series of increasing ethanol concentration (70%-100%), cleared in Histo-Clear and embedded in paraffin. The paraffin-embedded samples were sectioned sagittally at 5 µm thickness. The Bouin-fixed sections were stained with hematoxylin and eosin (H&E) for qualitative and quantitative assessment of liver parenchyma.

2.5.2 ApopTag staining

Apoptag®Plus Fluorescein In Situ Apoptosis Detection Kit was performed according to manufacturer's protocol (Chemicon) to detect DNA fragmentations which are associated with cellular apoptosis in the liver parenchyma. The blunt ends or single base overhangs

of 3'-OH ends in the fragmented DNA were labeled with the digoxigenin-nucleotide and then were bounded to anti-digoxigenin antibody (Anti-DIG) that is conjugated to alkaline phosphatase. The localizations of DNA fragmentations in apoptotic bodies were detected enzymatically with 5-Bromo-4-chloro-3-indolyl phosphate (BCIP)/Nitroblue tetrazolium (NBT) substrate.

Apoptag® staining was performed on formalin-fixed paraffin-embedded samples that were sectioned sagittally at 5 µm thickness.

2.5.3 Periodic acid-Schiff (PAS) staining

PAS is used to detect glycogen in tissue sections. Staining was performed on formalin-fixed paraffin-embedded sections using Alcian Blue PAS stain kit without diastase according to manufacturer's protocol (BioGenex).

2.5.4 Oil Red O staining

Oil Red O is used to stain for lipids. Fresh frozen liver samples were sectioned with Cryostat Sectioning and stained with Oil Red O (Sigma-Aldrich). Sections were also counterstained with hematoxylin for contrast.

2.5.5 Histological examination

Histopathological assessment was performed with a compound microscope, Axioskop 2 (Zeiss®), for T0901317-induced phenotypic changes in liver parenchyma at tissue level.

This assessment serves to corroborate transcriptomic profile generated from microarrays. Hematoxylin and Eosin-stained liver sections from treated and control fish were compared for qualitative (i.e. visible changes in liver parenchyma) and quantitative (i.e. hepatocytes nuclei density) changes. Density of the hepatocyte nuclei (no. of hepatocyte nuclei/7,250 μm^2) was measured in treated and untreated fish liver with the image analyzer program (Axiovision, Zeiss®). Each portion (anterior, middle and posterior regions) of the liver sections (1,000x magnification) of each liver from four experimental groups (control, T0901317 20 nM, 200 nM and 2,000 nM) were used to determine the density of hepatocytes nuclei, and three fields were counted for each liver portion from each replicate. Four (n=4 liver samples) biological replicates were assessed in each group. The statistical significance ($P<0.01$, $P<0.05$) of changes in density was determined using a heterocedastic t-test.

Images of H&E, apoptag, Oil Red O and PAS sections (200x and 1,000x magnification) were taken with Axioskop 2 for each liver from untreated and treated fish. Images which are most representative of liver parenchyma phenotype from each group are presented in the paper.

Chapter 3

Transcriptomic response to liver X receptor (LXR) agonist T0901317 in zebrafish liver

In our efforts to understand nuclear receptor-induced response and toxicity in the liver as well as to facilitate the use of zebrafish as a chemical biology model, we have employed transcriptomic approach to investigate T0901317-induced responses in the zebrafish liver to determine its potential as a model for LXR-related studies., Here we present histological and transcriptomic data capturing known effects of LXR agonists as reported in rodent models. This included up-regulation of LXR-targeted genes suggesting LXR activation, increased apoptotic activity in the liver and induced hepatic steatosis. Furthermore, our transcriptomic analysis provided additional insights into LXR activation which result in transcriptional suppression of the coagulation and complement pathways, insulin signaling pathways and possibly the induction of insulin deficiency that could contribute to known therapeutic and pathologic effects of LXR activation. Using a new batch of fish for quantitative real-time PCR, we confirmed that the genes associated with these biological processes were indeed down-regulated by T0901317-induced LXR activation in the liver suggesting that activated LXR may function as a transcription repressor of these processes.

3.1 Histological analysis of T0901317-induced effects and toxicity in zebrafish liver

Histological analysis was performed on the liver from male adult zebrafish exposed to a range of T0901317 concentrations to establish the appropriate concentration used for subsequent microarray experiment. All treatments and control groups had 0.05% (v/v) DMSO as vehicle. We observed that 20 nM, 200 nM and 2,000 nM of T0901317 caused

dose-dependent histological changes in the liver. We found that the T0901317-treated liver parenchyma appeared to be less homogenous and the hepatocytes were larger and less regular in shape as the T0901317 concentration increased when compared to the more compact, smaller and polygonal-shaped hepatocytes in the control group (Figure 1, a-d). Moreover, the number of hepatocyte nuclei as observed in the hematoxylin and eosin (H&E) stained sections, reduced significantly as T0901317 concentration increased (Figure 1e). Apoptag staining in the liver of T0901317-treated fish suggests increased apoptotic activity (Figure 1, g and h), which together with hepatocyte swelling as suggested by the larger cell-size appearance (Figure 1, a-d) had likely contributed to the apparent decreased in nuclei count. Oil-red O staining detected increased intracellular lipid accumulation in some hepatocytes by T0901317 treatment (Figure 1, i and 1j) suggesting hepatic steatosis as observed in rodents (Baranowski, 2008). Taken together, the histological analyses suggest a dose-dependent hepatotoxicity could be induced in adult male zebrafish exposed to 20 nM, 200 nM and 2,000 nM of T0901317; hence these concentrations were used for the subsequent microarray experiments. LXR activation was also confirmed by the up-regulation of a known LXR-targeted lipogenic fatty acid synthase-like *(fasn-like)* (Fig 1f), as determined by quantitative real-time RT-PCR using liver RNA from adult male fish exposed to 200 nM and 2,000 nM of T0901317. The up-regulation of fatty acid synthase by T0901317 is known to increase hepatic lipids as reported in rodents (Steffensen and Gustafsson, 2004) as also observed in our study (Fig 1, i and j). These findings confirmed that the zebrafish LXR was indeed activated by T0901317.

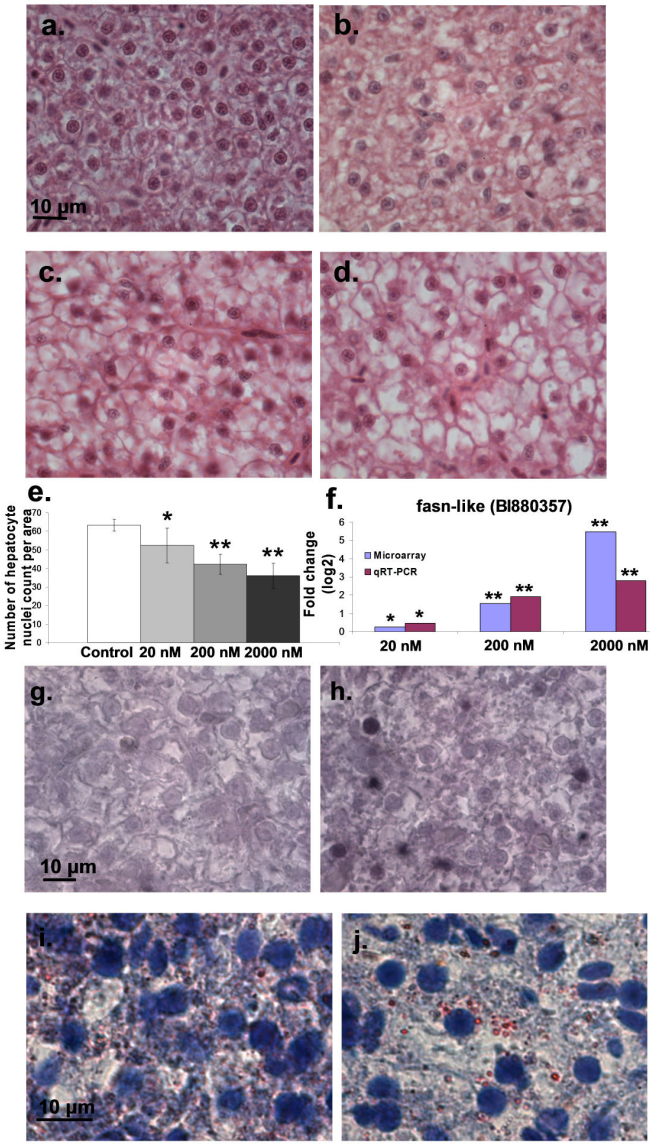

Figure 1. Hepatotoxicity induced by T0901317. (a-d) Hematoxylin and eosin (H&E) stained liver sections from adult male zebrafish exposed to (a) vehicle only (control, 0.05% DMSO), (b) 20 nM (c), 200 nM and (d) 2000 nM of T0901317. The livers from fish exposed to 200 nM and 2000 nM of T0901317 appeared less homogeneous and the hepatocytes are bigger and more irregular in shape compared to controls. (e) H&E stained liver sections from fish exposed to T0901317 compared to controls showed dose-dependent decrease in number of hepatocyte nuclei count per area section (dimensional area: 7250µm^2) (* p value<0.01, ** p value<0.05). (f) Fatty acid synthase-like (*fasn-like*), a liver x receptor targeted gene, displayed dose-dependent up-regulated gene expression (* p value<0.01, ** p value<0.05). (g) & (h) Liver cells from fish exposed to 2000nM of T0901317 showed increased staining for apoptosis-induced DNA breakage compared to control using Apoptag^{tm} staining kit. (i) & (j) Liver parenchyma from fish exposed to 2000nM of T0901317 showed increase lipid vesicles compared to control group using oil red O staining.

3.2 Microarray experiment and knowledge-based analysis of T0901317 Treatment

3.2.1 Trancriptome analysis of T0901317-induced liver responses with Gene Set Enrichment Analysis

For the microarray experiment, adult male zebrafish were exposed to T0901317 at 20 nM, 200 nM and 2,000 nM with 0.05% (v/v) DMSO as vehicle for 96 hours, whereas the control group was exposed to vehicle only. Five biological replicates were performed for each treatment group and each replicate consists of livers pooled from 4 individual male fish. Hence, for the three treatment groups and one control group, a total of 20 microarray hybridizations were performed on 20 pooled liver samples derived from 80 zebrafish.

The transcriptome data of each treatment group i.e. Low (L: 20 nM), Mid (M: 200 nM), High (H: 2000 nM) and in one combined analysis group [Low, Mid and High (LMH)] were compared to the control group using t-test to generate a *p*-value for each gene in the respective group. A ranking metric [$\log_{10}$ (1/*p*-value); assigned as 'positive' or 'negative' for up- or down-regulation, respectively] for each gene was generated to rank all the genes in the transcriptome data into a ranked list according to their statistical significance within the respective group for Gene Set Enrichment Analysis (GSEA) (Subramanian et al., 2005). GSEA utilizes Kolmogorov-Smirnov statistic to determine if a group of predefined Molecular Signature (total of 1892 curated gene sets) are significantly over-represented at the top or bottom of an entire ranked list of genes in each respective group of the T0901317-treated transcriptome profiles (See Materials and Methods). A

normalized enrichment score (NES) and a False Discovery Rate (FDR) value (corrected for multiple hypothesis testing) were generated for each of the molecular signature gene sets to represent the extent of the over-representation and its statistical significance, respectively. Negative and positive NES values indicate if the over-represented genes were mostly down- or up-regulated, respectively. Molecular signature with FDR<0.25 was considered as statistically significant in GSEA analyses (Subramanian et al., 2005). For the present study, we also considered those having 0.25≤ FDR <0.35 as marginally significant and those with FDR≥0.35 not significant. Based on the categories of FDR values and NES, profiles of the molecular signatures were analyzed and those that were marginally significant (FDR <0.35) in at least two of the concentrations (20 nM, 200 nM, 2000 nM and LMH) were represented in Figure 2. The GSEA analysis revealed that genes involved with molecular signatures associated with cellular morphology and adhesion, cellular stress-induced responses, coagulation cascade and complement system, beta-oxidation and diabetes were perturbed by LXR.

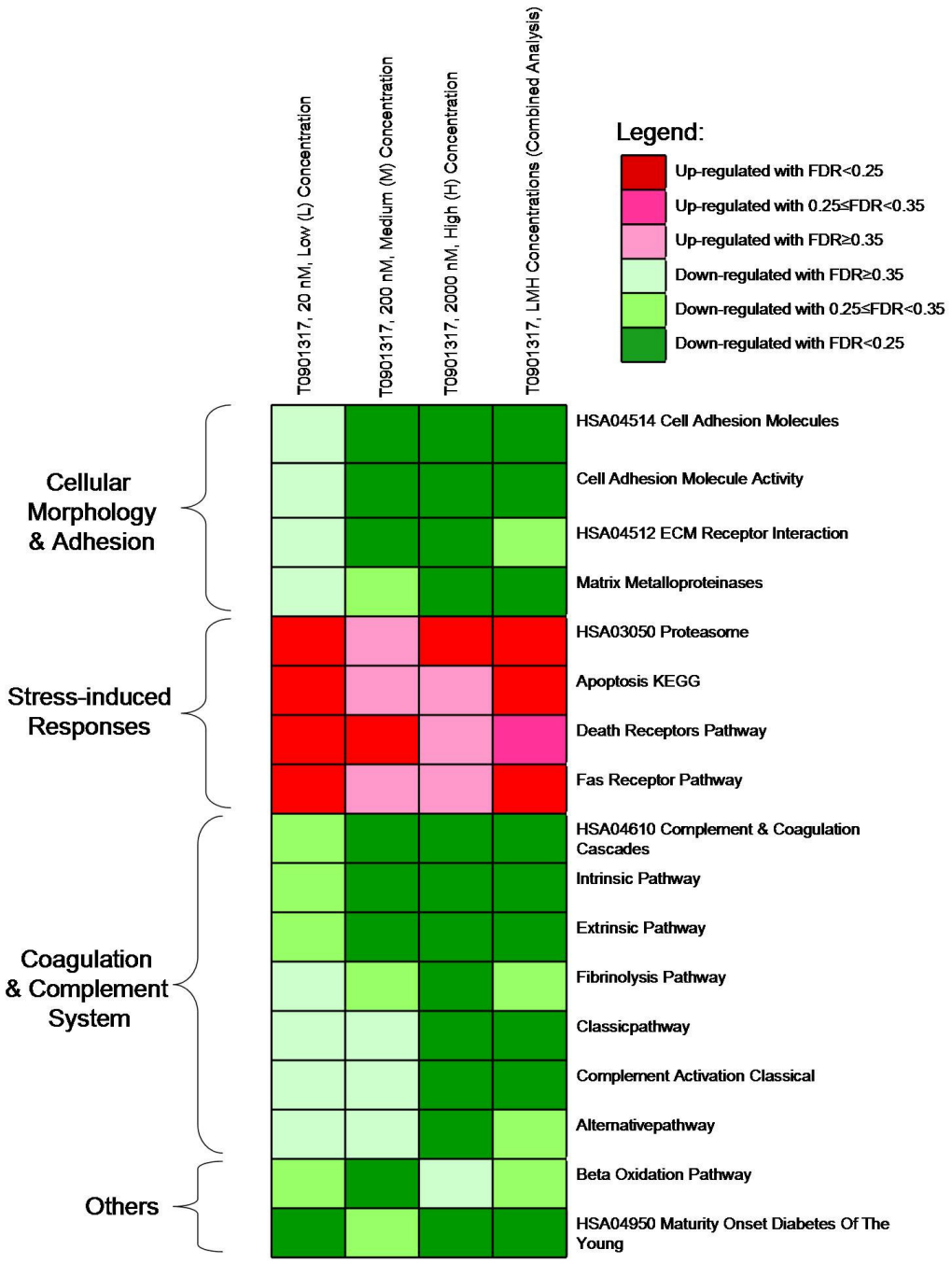

Figure 2 Gene Set Enrichment Analysis (GSEA) of liver transcriptome of T0901317-treated zebrafish. GSEA analysis is carried out on the transcriptome profile of the treatment groups 20 nM, 200 nM, 2000 nM, and combined Low, Mid and High (LMH) compared to control group. Significant deregulated molecular signature gene sets are grouped according to related processes: "Cellular Morphology & Adhesion", "Stress-induced Responses", "Coagulation & Complement System" and "Others". Up- and down-regulated gene sets are indicated in different shades of red and green, respectively. The shades of red and green are based on significance value of false discovery rate (FDR) (see figure legend).

3.2.1.1 Cellular Morphology and Adhesion

Based on our transcriptomic analysis, T0901317-induced LXR activation appeared to down-regulate dose-dependently molecular signatures associated with cellular morphology and adhesion which include Cell Adhesion Molecules (HSA04514), Cell Adhesion Molecule Activity, ECM Receptor Interaction (HSA04512) and Matrix Metalloproteinases (MMPs). Modulations of these molecular signatures were likely associated with the histological changes in cell and tissue morphology observed in the liver. Interestingly, LXR has been proposed as a potential therapeutic target for atherosclerotic therapy (Repa and Mangelsdorf, 2002) and T0901317-induced LXR activation has been shown to suppress the expression of cellular adhesion molecules in atherogenic vascular tissues (Verschuren et al., 2009). Moreover, it has been reported that inhibition of broad-spectrum of matrix metalloproteinases (MMPs) leads to reduction in atherogenic progression (Baker et al., 2002; Prescott et al., 1999). Interestingly, we have captured down-regulation of molecular signature involving MMPs in the zebrafish liver suggesting that suppression of MMPs expression by LXR could be a contributing factor to the anti-atherogenic action as reported in the rodent study (Verschuren et al. 2009). It is encouraging to note that the down-regulation of signatures associated with cellular morphology and adhesion that are known to be associated with the therapeutic anti-atherogenic action of LXR activation, can be captured by our transcriptomic analysis of T0901317-induced acute response in the zebrafish liver. This further highlights its potential for drug screening.

3.2.1.2 Coagulation and complement systems

We also observed in our analysis that LXR activation by T0901317 down-regulated some molecular signatures associated with coagulation and complement system including HSA04610 Complement & Coagulation Cascades, Intrinsic Pathway, Extrinsic Pathway, Fibrinolysis Pathway, Classic Pathway and Complement Activation Classical Pathway. One of the negatively enriched signature, HSA04610 Complement & Coagulation Cascades, showed that with increasing T0901317 concentrations, normalized enrichment score and *p*-value decrease, thereby suggesting that T0901317 induces dose-dependent down-regulation (Figure 3, a-c). By examination of expression levels of 31 genes involved in the pathway, we have found that all of them are down-regulated with increasing concentrations of T0901317 (Figure 3d), indicating that LXR may affect expression of these genes and thus may be involved in the complement and coagulation cascades pathway. We verified the association of LXR activation with complement and coagulation cascades in literature.

LXR activation has been shown to suppress the gene expression and/or protein level of tissue factor (TF), a major initiator of blood coagulation (Camerer et al., 1996), in human islets (Scholz et al., 2009) and mouse macrophages (Terasaka et al., 2005). Macrophages are major source of TF that contributes to thrombogenesis in atherosclerosis (Terasaka et al., 2005). Hence anti-thrombotic action via suppression of TF expression is one of the anti-atherosclerotic actions of LXR activation (Joseph et al., 2002). Interestingly, our data indicate LXR also suppressed expression of various genes (*pros1, f10, tfpi, serpinc1* and

plg) involved in the coagulation pathway that could further contribute to its anti-thrombotic action.

Additionally, activation of LXR by T0901317 was observed to down-regulate genes associated with the complement pathway which is part of innate immune system that could activate inflammatory response. Chronic inflammation also contributes to atherogenesis (Glass and Witztum, 2001; Lusis, 2000) and there are evidence that complement activation plays a major role in chronic inflammation that is associated to initiation and progression of atherosclerotic lesions (Niculescu and Rus, 1999) and also in rheumatoid arthritis (Okroj et al., 2007). Thus LXR-induced down-regulation of complement pathway, as shown in our data, can in turn suppress inflammatory responses and therefore promote anti-atherogenic effect (Zelcer and Tontonoz, 2006), and also ameliorate rheumatoid arthritis (Chintalacharuvu et al., 2007). Therefore LXR-induced down-regulation of complement pathway in our data suggests that LXR could further modulate the inflammation and innate immune system in zebrafish.

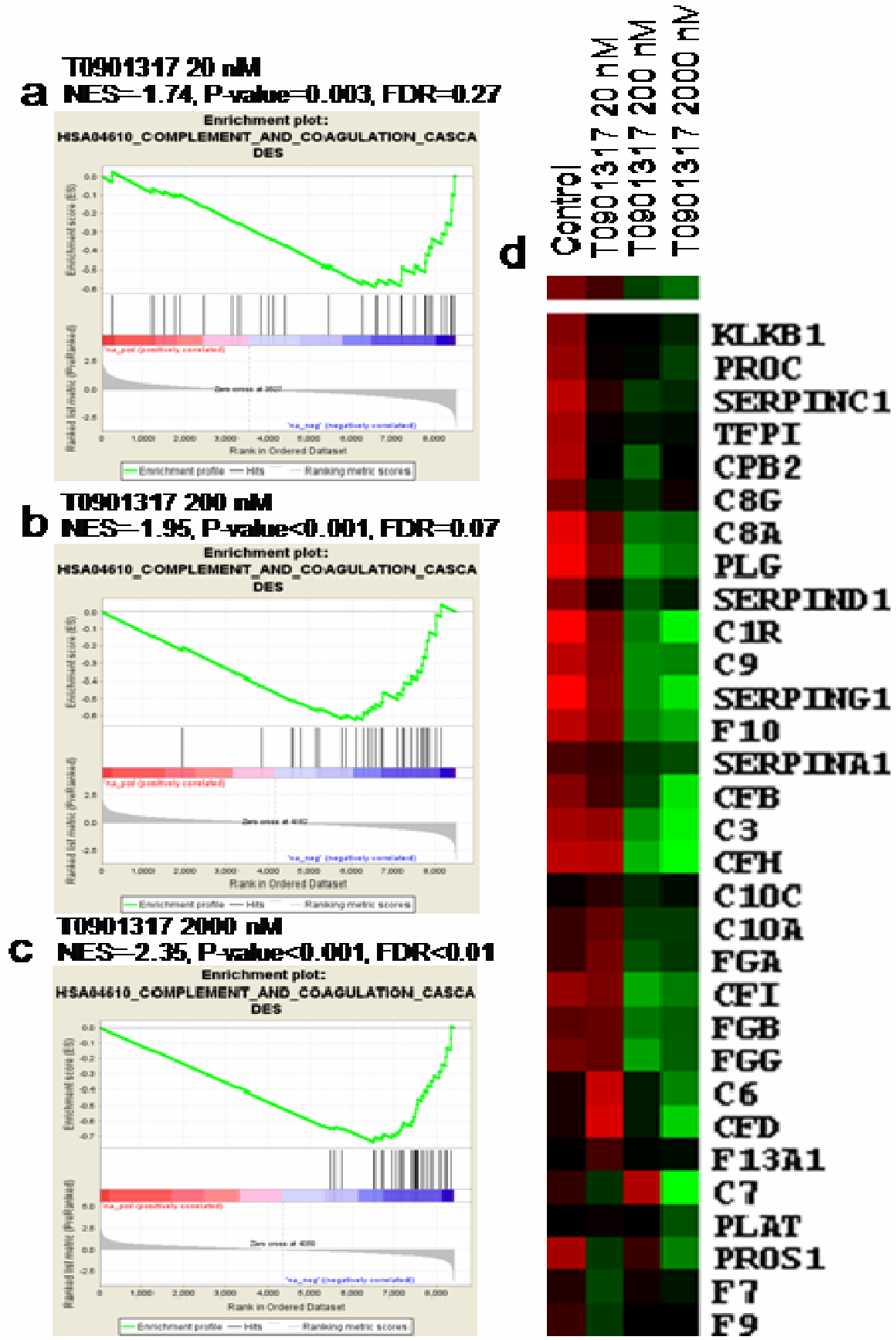
a
T0901317 20 nM
NES=-1.74, P-value=0.003, FDR=0.27
Enrichment plot:
HSA04610_COMPLEMENT_AND_COAGULATION_CASCADES
b
T0901317 200 nM
NES=-1.95, P-value<0.001, FDR=0.07
Enrichment plot:
HSA04610_COMPLEMENT_AND_COAGULATION_CASCADES
c
T0901317 2000 nM
NES=-2.35, P-value<0.001, FDR<0.01
Enrichment plot:
HSA04610_COMPLEMENT_AND_COAGULATION_CASCADES
Rank in Ordered Dataset
Enrichment profile
Hits
Ranking metric scores
d
Control
T0901317 20 nM
T0901317 200 nM
T0901317 2000 nM
KLKB1
PROC
SERPINC1
TFPI
CPB2
C8G
C8A
PLG
SERPIND1
C1R
C9
SERPING1
F10
SERPINA1
CFB
C3
CFH
C10C
C10A
FGA
CFI
FGB
FGG
C6
CFD
F13A1
C7
PLAT
PROS1
F7
F9

Figure 3. Gene set enrichment analysis (GSEA) of the dose-dependent transcriptional suppression by T0901317 treatment on complement and coagulation cascade pathway. Three different concentrations of T0901317, 20 nM (**a**), 200 nM (**b**), and 2000 nM (**c**), were used for treatment. Normal enrichment score (NES), *p*-values, and false discovery rate (FDR) for "Complement and Coagulation Cascade" gene set decrease as the treatment concentration increases, suggesting that T0901317 induced a dose-dependent down-regulation of this pathway. (**d**) Expression levels of 31 zebrafish genes mapped to the gene set of this pathway. All of these genes were down-regulated with increasing concentration of T0901317.

3.2.1.3 Cellular toxicity and stress-induced Reponses

Several molecular signatures associated with stress responses and/or cytotoxicity were induced by LXR activation. This may be related to protein and DNA damage and subsequently cell death as evident by the up-regulation molecular signature such as proteasome (HSA03050), apoptosis, death receptors pathway and Fas receptor pathway. Increased apoptotic activity is in liver was confirmed with Apoptag staining (Figure 1, g and h). LXR activation by T0901317 has been reported to induce apoptosis in pancreatic beta cells (Choe et al., 2007) and more recently has been shown to exert anti-proliferative effect via cytotoxicity and apoptosis in ovarian (Rough et al., 2010) and prostate (Pommier et al., 2006) cancer cells. Our data suggests that LXR-induced apoptosis in liver may be mediated by Death Receptor Pathway and FAS Receptor Pathway.

3.2.1.4 Diabetes and Beta-oxidation of Fatty Acids

The down-regulated molecular signatures by LXR activation also included Maturity onset Diabetes of the Young (MODY) and Beta-oxidation Pathway. LXR is known to exert effects on major carbohydrate and lipid metabolic pathways (Baranowski, 2008). MODY is an autosomal dominant monogenic form of type II diabetes characterized by insulin resistance and relative insulin deficiency. Genes listed in the molecular signature are implicated in MODY afflicted carriers due to gene mutations. Down-regulation of genes associated with MODY suggests that LXR-induced perturbation that promotes insulin resistance and/or insulin deficiency. Down-regulation of beta-oxidation pathway, where

fatty acids are catabolized to generate energy, may be associated with increased hepatic lipogenesis as evident by intracellular lipid accumulation in liver of fish treated with T0901317 (Figure 1, i and j). There is evidence for impaired beta-oxidation promotes hepatic steatosis (Wei et al., 2008). It has been reported that chronic (3-6 days) *in vitro* activation of LXR by T0901317 induced apoptosis of pancreatic beta cells through hyperactivation of lipogenesis and this could lead to insulin deficiency and promote diabetes (Choe et al. 2007). More recently, LXR activation in human islets resulted in lower basal insulin secretion is concordant with the decreased insulin expression in our data (Scholz et al., 2009). Additionally Basciano et al. (2009) has reported that LXR activation by T0901317 via oral gavage for 4-7 days could stimulate hepatic lipoproteins production but also induced insulin resistance through reductions in insulin signaling in male Syrian golden hamster, which is contrary to previous findings that on antidiabetic role for LXR agonists (Cao et al., 2003; Grefhorst et al., 2005; Steffensen and Gustafsson, 2004). The contrasting result could be due to the differences in the animal models used; most reported anti-diabetic actions via LXR activation by T0901317 were observed in diabetic animal models (Cao et al., 2003; Grefhorst et al., 2005; Steffensen and Gustafsson, 2004), while Basciano et al. (2009) and we used non-diabetic animals. Given the difference in metabolic state between diabetic and non-diabetic livers, the contrasting findings were not surprising but interesting to warrant further investigation. Basciano et al. (2009) has proposed the possibility of LXR activation as a causative factor in the induction of insulin resistance through decrease insulin signaling, and that chronic LXR agonist treatment (2-4 weeks) may lead to more profound signaling changes and induction of an insulin-resistant state in the liver. Similarly, we have observed down-

regulation of insulin signaling (*ins, irs2, irs*) (see discussion on Figure 4 below and Table 3). It was also reported that pancreatic islets of several diabetic rodent models have significant elevated LXR expression, and it has been suggested that chronic LXR activation could contribute to β-cell dysfunction and eventually diabetes (Choe et al., 2007). Therefore in line with the use of zebrafish for disease modeling, it would be interesting albeit requiring further study, to investigate the possibility of chemically-induced a diabetic model in zebrafish via LXR activation by T090131.

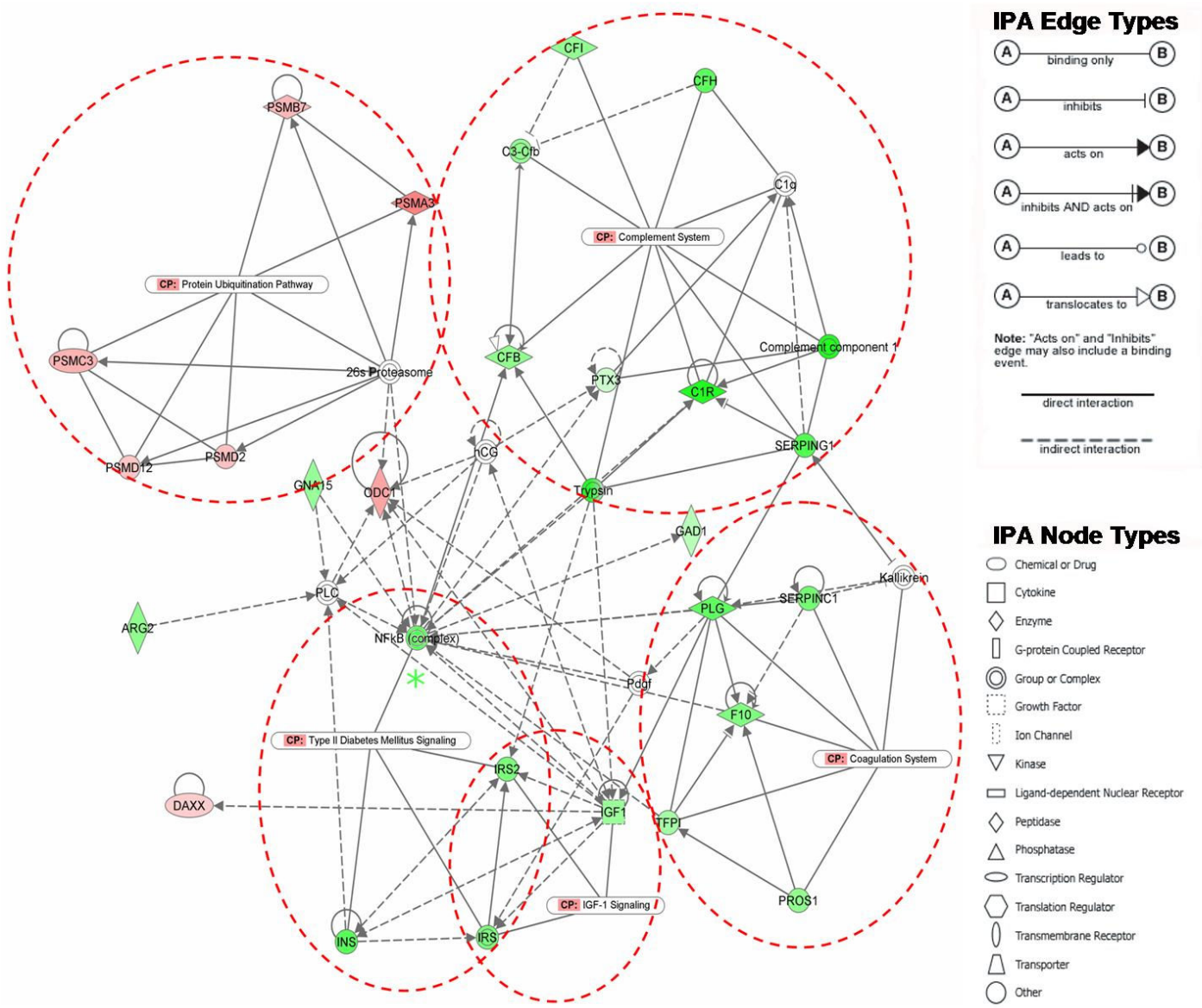

Figure 4. Gene network analysis of liver X receptor activation for biological inferences. Top network for LXR activation was generated with Ingenuity Pathway Analysis (IPA) software. Up- and down-regulated molecules are in red and green symbols, respectively. Non-coloured genes are either not present on microarray probes or not significant in the combined Low, Mid and High (LMH) concentrations compared to controls, but are included by IPA to maximize the connectivity of deregulated genes. NF-kB (complex) is coloured green and marked with (*), since our validation showed down-regulation of *REL* homolog (Table 3), one of the subunits of NF-kB complex. These genes are grouped (as highlighted in red-dotted circle) into several canonical processes: "Protein Ubiquitination Pathway", "Complement System", "Coagulation System", "Type II Diabetes Mellitus Pathway" and "IGF-1 (insulin-like growth factor 1) pathway".

3.2.2 Insights from Biological Network Analysis

We examined the top connected network generated by IPA using 57 human homologs that are leading edge genes as identified by GSEA in selected canonical pathways (Figure 2) and are statistically significant (t-test, $p<0.05$) in LMH treatment group compared to controls. A top network (Figure 2) consisting of 36 human homologs (25 homologs from our microarray data) clustered into four major canonical pathways (coagulation system, protein ubiquitination pathway, complement system and insulin receptor signaling) was generated. Interestingly, insulin-like growth factor 1 (IGF1) signaling cluster was observed in the network suggesting modulation by LXR activation. We validated the down-regulation of IGF-1 gene expression with quantitative real-time PCR (Table 3). It was also previously reported that LXR activation with T0901317 suppressed IGF1 expression in female rat hepatocytes (Kotokorpi et al., 2004). Therefore LXR activation may suppress IGF1-mediated growth signaling.

In the network, SERPING1 from the complement system and PLG from the coagulation system are shown to be linked together, which provides insight into the mechanism of LXR activation in modulating these two processes (Figure 4). There are evidence that complement and coagulation system interact and crosstalk between each other since several studies have shown that initiation of complement or coagulation pathways can potentiate or trigger each other's activation mutually (Amara et al., 2008; Markiewski et al., 2007). Hence LXR activation is also likely to suppress complement and coagulation systems via diminishing mutual initiation between the two systems.

Molecules from coagulation (SERPINC1, PLG, F10 and TFPI) and complement (CFB, Trypsin and C1R) system are also linked to NF-kB complex, a protein complex that regulates immune and inflammatory response. LXR activation is known to perturb NF-kB signaling by inhibiting expression of NF-kB target genes (Castrillo et al., 2003; Cheng et al., 2010; Wu et al., 2009). Castrillo et al. (2003) suggested that repression of NF-kB target genes occurs via downstream of NF-kB binding to DNA, whereas Cheng et al. (2010) showed that it occurred via preventing translocation of p65 from cytoplasm to nucleus. NF-kB directly regulates TF transcriptionally to promote thrombotic action (Mackman, 1997) and there is evidence that NF-kB activation could lead to complement activation (Korbelik, 2009). There are also evidence that deregulation in NFkB activation leads to atherosclerosis (Van der Heiden et al., 2010) and rheumatoid arthritis (Simmonds and Foxwell, 2008). Hence, NFk-B was proposed as a therapeutic target to treat these ailments (Simmonds and Foxwell, 2008, Van der Heiden et al., 2010). We validated the down-regulation of *REL homolog*, one of the five identified subunits of NFkB, gene expression (Table 3). Our result suggests that LXR activation could suppress *REL* homolog, and therefore perturbs NF-kB signaling. Subsequently, this induces attenuation of coagulation and complement system.

Although there had been reports that LXR activation exerts anti-thrombogenic, anti-atherogenic and anti-inflammatory effects, our study provided additional mechanistic insights. Taken together, our study revealed that LXR may be functioning as a transcriptional repressor of the coagulation and complement systems that could partly contribute to anti-atherogenic and anti-inflammatory effects of LXR activation reported

in rodent studies (Chintalacharuvu et al., 2007; Joseph et al., 2002; Li et al., 2010; Peerschke and Ghebrehiwet, 2010; Repa and Mangelsdorf, 2002). We observed that genes involved in this network of pathways to be significantly down-regulated. While transcriptional repression of the coagulation and complement systems by LXR activation has not been reported previously, transcriptional repression by LXR on genes implicated in inflammation and lipid metabolism has been described (Blaschke et al., 2006; Ghisletti et al., 2009; Jakobsson et al., 2007; Scholz et al., 2009; Wang et al., 2008). Majority of LXR-induced repression of genes involved with inflammatory signaling pathways in macrophages was shown to require transrepression by nuclear receptor corepressor (NCor) and silencing mediator of retinoic acid and thyroid hormone receptor (SMRT) corepressors (Ghisletti et al., 2009). Complement activation promotes inflammation and coagulation (Peerschke and Ghebrehiwet, 2010), hence it is plausible that LXR activation may transrepress complement activation and coagulation that is mediated by NCor and SMRT.

While genes in the protein ubiquitination cluster were up-regulated, genes in insulin receptor signaling cluster were suppressed. Ubiquitin-proteasome system is implicated with diabetes, as shown from one study that proteasomal activity was elevated in muscles of acute insulin-deficient diabetic rats (Lecker et al., 1999). Insulin regulates cellular protein turnover by inhibiting protein degradation in adult animal (Rooyackers and Nair, 1997). This inhibitive effect promotes conservation of protein stores during availability of other energy substrates (e.g. carbohydrates), and inversely when insulin level is low (e.g. during starvation) there is promotion in breakdown of amino acids for

gluconeogenesis (Fawcett et al., 2001) Hence low insulin signaling could have elevated proteasome activity in the liver (Figure 3) (Fawcett and Duckworth, 2009). Taken together, it is plausible that LXR activation induced suppressed insulin level, as suggested by decreased insulin (*ins*) expression (Table 3), and this would subsequently enhance proteasomal degradation, as suggested by up-regulation in protein ubiquitination cluster (Fig. 3). Thus, LXR activation may promote proteasome activity by decreasing insulin level in the liver.

Table 3. *Quantitative real-time PCR validation for selected genes in T0901317 treatment.*

		Log2(fold-change) Expression					
		200 nM		2000 nM		200 nM & 2000 nM	
Gene Symbol	**Genbank ID**	**Array**	**qRT-PCR**	**Array**	**qRT-PCR**	**Array**	**qRT-PCR**
Known LXR Target Genes							
lxr	BC092160	NA	**1.55	NA	**1.40	NA	**1.45
fasn	AW077199	NA	**1.93	NA	**2.67	NA	**2.48
Cellular Morphology Adhesion							
vcam1	AW344246	**-2.55	-0.31	-1.78	**-0.79	*-2.19	**-0.55
mmp9	AW174507	-0.04	**-1.07	-0.05	**-3.14	*-0.05	**-1.95
itga9 homolog	BC054897	-1.12	**-0.93	-0.93	**-0.89	* -1.03	**-0.90
Coagulation Cascade							
f10	BM154293	-4.52	**-2.70	* -4.81	**-0.63	**-1.44	**-1.13
pros1 homolog	BI887609	-1.25	**-1.14	**-1.89	**-1.66	** -4.67	**-1.43
Fibrinolysis							
plg	BC059801	-11.48	**-1.01	-10.92	**-1.11	** -11.20	**-1.07
Complement System							
c8a	AW018673	-9.34	**-0.66	-9.09	**-0.85	** -9.21	**-0.76
c9	AW019201	-11.19	**-1.68	-11.02	**-2.14	**-11.11	**-1.91
Beta-Oxidation							
acads	BC079521	-1.24	**-0.93	*-1.30	**-1.39	**-1.27	**-1.21
Gluconeogenesis							
g6pca	BC076446	** -8.58	*-0.43	*-8.54	**-1.09	**-8.56	**-0.79
Insulin Growth Factor 1 Signaling							
igf1	AF268051	-4.17	0.08	*-4.25	**-3.32	**-4.21	**-1.15
Maturity Onset Diabetes of the Young							
hnf1ba	AF430840	0.03	*-0.66	*-0.63	-0.46	-0.33	*-0.55
ins	AF036326	**-1.88	-2.09	-1.70	*-3.74	**-1.80	*-2.89
Nuclear Factor Kappa-light-chain-enhancer Of Activated B Cells							
rel homolog	BC076403	0.01	-0.17	-0.10	**-1.16	-0.05	**-0.78

The genes were selected based on biological function of interest identified by GSEA. The relative $\log_2$ fold-change above controls as determined by quantitative real-time polymerase chain reaction (qRT-PCR) and microarray (Array) are presented (* p-value <0.1; ** p-value < 0.05).

3.3 Validation of gene expression via quantitative real-time PCR

We also confirmed the deregulated biological processes identified in our transcriptomic analysis by validating expression levels of relevant genes with real-time PCR in another batch of newly-treated zebrafish under the same experimental conditions. As shown in Table 3, the expression of 14 genes were validated: *vcam1* (vascular cell adhesion molecule 1), *mmp9* (matrix metallopeptidase 9), *itga9*, (integrin, alpha 9 homolog), *f10* (coagulation factor X), *pros1* [protein S (alpha) homolog], *plg* (plasminogen), *c8a* (complement component 8, alpha polypeptide), c9 (complement component 9), *acads* (acyl-Coenzyme A dehydrogenase, short chain), *g6pca* (glucose-6-phosphatase a, catalytic), *igf1* (insulin-like growth factor 1), *hnf1ba* (HNF1 homeobox Ba), *ins* (insulin) and *rel* (reticuloendotheliosis viral oncogene homolog). All of these genes showed significant difference in expression in the presence of T0901317 were significant ($p < 0.10$) at combined highest and lowest (T0901317 2000 nM & 200 nM) concentrations (Table 3). These 14 genes confirmed down-regulation of the following biological processes in the liver of fish exposed to T0901317: cell adhesion and tissue structure (*vcam1, ITGA9* homolog), matrix metalloproteinases (*mmp9*), coagulation cascade (*f10, PROS1* homolog), fibrinolysis (*plg*), complement pathway (*c8a, c9*), beta-oxidation pathway (*acads*), gluconeogenesis (*g6pca*), IGF-1 (*igf1*) signaling pathway, MODY (*ins, hnf1ba*) and NF-kB signaling (*REL* homolog). Hence, this second experiment using a new batch of T0901317-treated fish was corroborated with our transcriptomic experiment and GSEA analysis as well as histological analysis in earlier experiments. The up-regulation of LXR targeted genes, *fasn, fasn-like* and *lxr* itself confirming the LXR

activation which can act as a transcriptional repressor of these biological processes. This in turn may contribute to the effects of LXR activation as reported in rodent models, be it therapeutic effects (e.g. anti-thrombogenic, anti-atherogenic and anti-inflammatory actions) or pathologic effects (e.g. steatosis and insulin deficiency). For example, MMP9 is implicated in promoting atherogenesis in arteries via vascular vessel remodeling (Mason et al., 1999) and down-regulation of *mmp9* validated in our study (Table 3) may contribute to the anti-atherogenic action of LXR agonist. Furthermore, NF-kB signaling, which regulates immune system and inflammation, is suggested to be perturbed from the down-regulation of *REL homolog* (Table 3), one of the subunits of NF-kB complex. Thus this may contribute to the anti-inflammatory action. Likewise, LXR activation is known to inhibit hepatic gluconeogenesis (Baranowski, 2008). The expression of *g6pca*, which encodes one of the rate-limiting enzymes of gluconeogenesis, was down-regulated in our experiment (Table 3). Loss of G6PC function is involved with excessive accumulation hypertriglyceridemia and hepatic steatosis (Hutton and O'Brien, 2009), hence the suppression of *g6pca* expression could promote increase lipid levels as observed in our zebrafish liver (Figure 1, i and j).

3.4 Conclusion

In conclusion, we demonstrated the potential of using zebrafish liver coupled with transcriptomic analysis to capture pharmacological and toxicological/pathological actions of LXR activation by an agonist T0901317. We were able to capture known effects of LXR activation as reported in mammalian models, suggesting conserved mode-of-actions

resulting from LXR activation between mammals and fish. We observed LXR activation led to transcription repression of several biological processes. To this, we were able to identify previously unknown transcription repression of genes associated with cell adhesion, coagulation and complement systems that could contribute to the anti-thrombogenic, anti-atherogenic and anti-inflammatory actions of LXR activation. In addition, we were able to identify and validate deregulated genes associated with insulin signaling, lipid and glucose metabolisms that could lead to hepatosteatosis and potentially insulin deficiency. Our findings place zebrafish as a suitable model for screening prospective LXR drug targets, LXR disruptors and investigating LXR-related metabolic disorders.

Chapter 4

Transcriptomic response to retinoic acid receptor (RAR) agonist all-trans retinoic acid in zebrafish liver

Here we investigated ATRA-induced responses in adult male zebrafish liver. We performed acute ATRA treatment to zebrafish at concentration that displayed hepatotoxic phenotype according to histological examination. Additionally two lower concentrations were performed to determine dose-dependent responses. This is followed by transcriptomic profiling of the livers with microarrays. Subsequently we compared transcriptomic profiles of untreated and treated livers through human homology mapping and knowledge-based data mining, to elucidate ATRA-induced responses. Histological and transcriptomic analysis were mutually corroborated through phenotypic anchoring. We performed comparative transcriptomic meta-analysis of ATRA-induced biological responses between zebrafish liver and mouse embryonic bodies, and found conserved responses between both models in fatty acid oxidation and proteasomal degradation, but also differential response in processes associated with immune system. We observed that ATRA induced up-regulation in immune response in zebrafish liver but down-regulation in embryonic bodies may be due to absence of immune cells in embryonic bodies. Thus this highlights zebrafish as a feasible in vivo model to study drug-induced responses. Furthermore, we validated deregulated biological processes in zebrafish with gene markers in a subsequent separate batch of treatment using quantitative real-time PCR.

4.1 Histological analysis of all-trans retinoic acid-treated liver

Appropriate ATRA-induced hepatotoxicity concentrations were determined according to the histological results of the adult male zebrafish liver treated for 96 hours, before performing the microarray experiment. The commonly used low ATRA concentration to

modulate zebrafish embryonic development is 20 nM (Nadauld et al., 2005; Hans and Westerfield, 2007), which is higher than the earlier reported physiological concentrations in serum of both pregnant humans (7nM; van Vliet et al., 2001) and red seabream fish (13.3 nM; Ogata & Oku, 2001). Thus 20 nM was selected as the lowest ATRA concentration, followed by two higher concentrations (200 nM and 2,000 nM). Histological analysis revealed dose-dependent changes in liver parenchyma: decreasing compactness and increasing size and irregular shape of hepatocytes (Figure 5, a-d). We also found increased apoptotic activity in the ATRA-treated liver parenchyma compared to the control using apoptag staining which stains for fragmented DNA (Figure 5, g and h), suggesting that increased apoptotic activity could have led to dose-dependent decrease in the density of hepatocytes nuclei in liver parenchyma (Figure 5e). Hepatic glycogen was shown to be elevated in treated liver compared to controls with Periodic acid-Schiff stain (Figure 5, i and j), which is concordant with a study that had reported increased glycogen accumulation in 5-day ATRA-treated human hepatocellular carcinoma cells (Piao et al., 2003). Furthermore, the amount of hepatic lipid vesicles increased in a dose-dependent manner (Figure 5, k-n), and this is concordant with a study that showed 2-day treatment with hypervitaminosis A led to fatty liver in young rats (Singh and Singh, 1978).

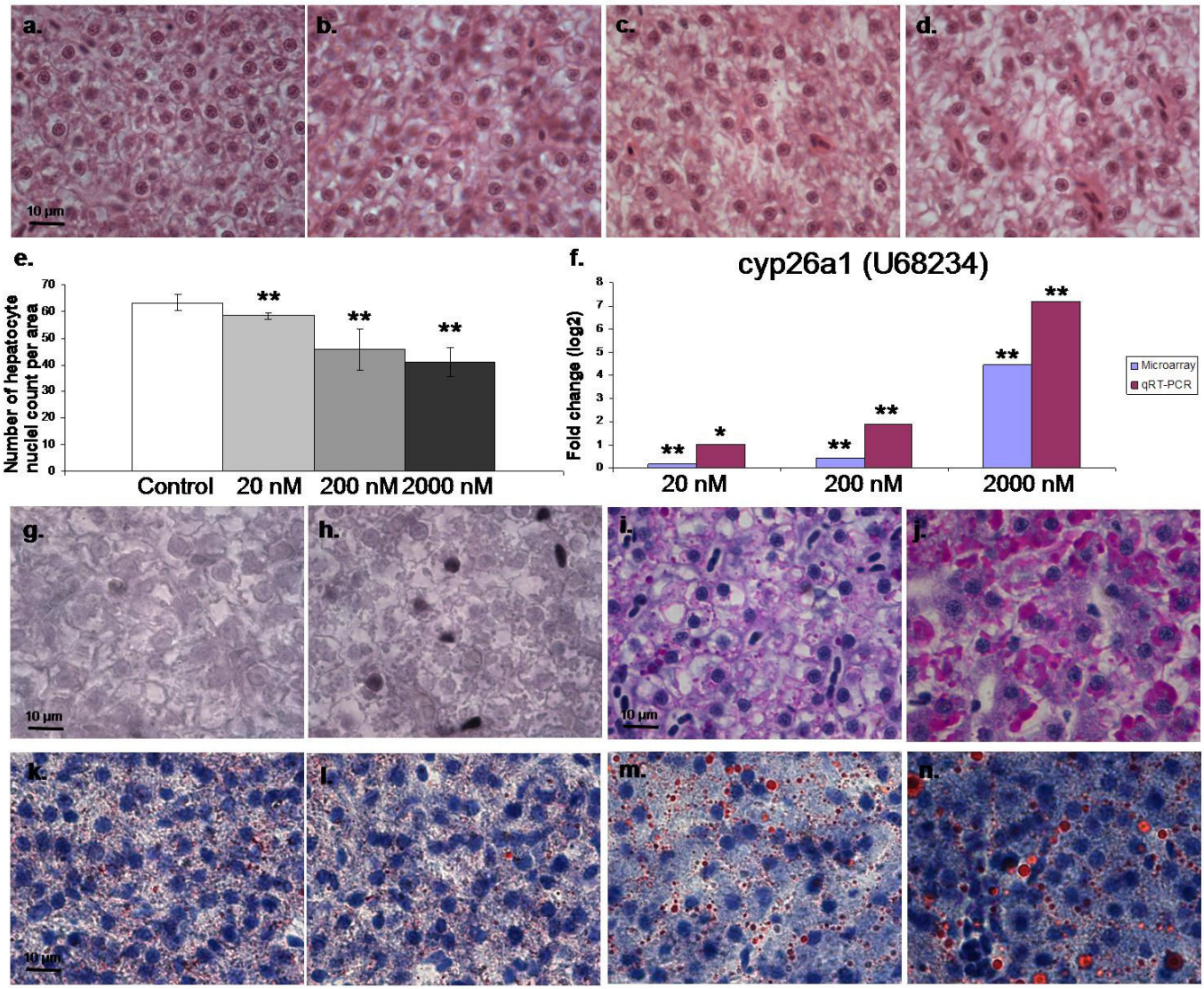

Fig 5. Hepatoxicity induced by all-trans retinoic acid (ATRA). (a-d) Hematoxylin and eosin (H&E) stained liver sections from adult male zebrafish exposed to (a) vehicle only (control, 0.05% DMSO), (b) 20 nM (c), 200 nM and (d) 2000 nM of ATRA. The livers from fish exposed to 200 nM and 2000 nM of ATRA showed decreasing compactness and increasing size and irregular in shape compared to controls. (e) H&E stained liver sections from fish exposed to ATRA compared to controls showed dose-dependent decrease in number of hepatocyte nuclei count per area section (dimensional area: 7250µm^2) (* p value<0.05, ** p value<0.01). (f) Cytochrome P450 26A1 (*cyp26a1*), a retinoic acid receptor targeted gene, displayed dose-dependent up-regulated gene expression (* p value<0.05, ** p value<0.01). (g) & (h) Liver cells from fish exposed to 2000nM of ATRA showed increased staining for apoptosis-induced DNA breakage compared to control using Apoptag^{tm} staining kit. (i) & (j) Hepatic glycogen showed increase compared to control group using periodic acid-schiff staining. (k-n) Liver parenchyma from fish exposed to 2000nM of T0901317 showed increased lipid vesicles compared to control group using oil red O staining.

4.2 Microarray experiment and knowledge-based analysis of all-trans-retinoic treatment

4.2.1 Microarray experiment and data normalization

In our microarray experiment, the adult male zebrafish were treated with ATRA at different concentrations [2000 nM, 200 nM and 20 nM with 0.05% (v/v) DMSO as vehicle] for 96 hours, and the control group was only exposed to the vehicle. The RA 200 nM group had four biological replicates, whereas all other treatment groups had five biological replicates. Each replicate is composed of pooled livers from four male zebrafish. Therefore, for the three treatment groups and one control group, 19 microarrays hybridization were performed using 19 pooled liver samples from 76 zebrafish.

Microarray data were analyzed by comparing each of the three concentration groups [Low (L:20 nM), Mid (M:200 nM), High (H:2000 nM)] and combined analysis of the three groups [20 nM, 200 nM and 2000 nM (LMH)] with the control group using t-test that will generate a *p*-value for each gene in each groups. Each gene was assigned a ranking metric [$\log_{10}$ (1/*p*-value; positive or negative values were designated based on up- and down-regulation, respectively] and ranked in a list according to the statistical significance in each respective group for Gene Set Enrichment Analysis (GSEA). GSEA uses Kolmogorov-Smirnov statistic to reveal if any set of predefined molecular signature (1,892 curated gene sets) has significant over-representation at the top or bottom of an entire ranked list of genes from ATRA-treated transcriptome profiles (see Materials and

Methods). A normalized enrichment score (NES) and a false discovery rate (FDR) value (corrected for multiple comparisons) are calculated for each molecular signature gene set to respectively designate the level of over-representation and its statistical significance. Negative and positive NES values indicate whether the genes are mostly over-represented as down- or up-regulated respectively. Subramanian et al. (2005) recommend signatures with FDR <0.25 as statistically significant, additionally we deem those having 0.25≤ FDR<0.35 as marginally significant and those having FDR≥0.35 as insignificant. In order to capture dose-dependent effect, we focused on selected gene sets that has FDR<0.35 in at least two of the concentrations (2000 nM, 200 nM and 20 nM) and FDR<0.25 in the combined LMH group of FDR<0.25. These selected gene sets were then presented in Figure 6 based on category of FDR values and whether NES value is positive (shades of red) or negative (shades of green).

Our transcriptome analysis revealed that genes associated with several biological processes were affected by ATRA: cytoskeletal assembly and reorganization, oxidative phosphorylation, oxidative stress-induced responses, cell death, protein and fatty acid metabolism, and immune responses.

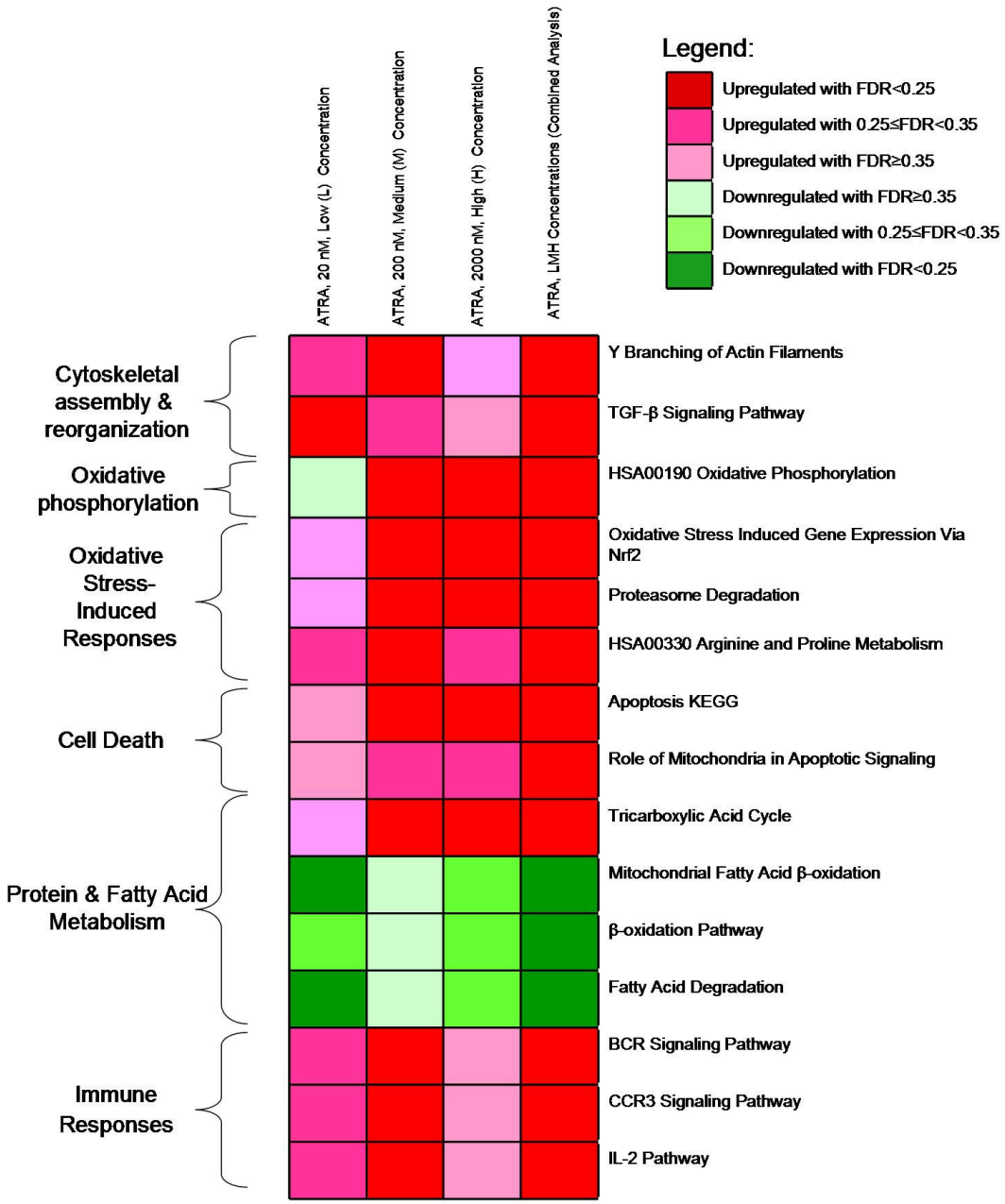

Fig 6. Gene Set Enrichment Analysis (GSEA) of liver transcriptome upon exposure to all-trans retinoic acid. GSEA analysis is performed on transcriptome profiles of 20 nM, 200 nM, 2000 nM and all combined three concentrations (20 nM, 200 nM and 2000 nM) of ATRA treatment groups (LMH) compared to control group. Significant dysregulated molecular signature gene sets are clustered according to related processes: "Cytoskeleton", "Oxidative Phosphorylation", "Oxidative Stress-Induced Responses", "Cell Death", "Protein & Fatty Acid Metabolism" and "Immune Responses". Up- and down-regulated gene sets are indicated as different shades of red and green respectively. The shades of red and green are based on the significance of false-discovery rate (FDR) (see figure legend).

4.2.2 Cytoskeletal assembly and reorganization

ATRA treatment modulated pathways involved in actin filament remodeling: Y branching of actin filaments. The actin remodeling pathways, mediated through actin related protein (Arp) 2/3 complex, may contribute to the irregular shape in the hepatocytes (Figure 5, a-d). Hypervitaminosis A is associated with HSC activation in patients (Nollevaux et al., 2006). Activated HSCs are suggested to be involved in modulating actin polymerization via myosins, which consequently change cell shape (Reynaert et al., 2008). HSC is suggested to be present in all vertebrates (Nollevaux et al., 2006) and it has been reported to be present in lamprey, eel, hagfish and teleost fish (cod and arrowtooth halibut) (Blomhoff and Wake, 1991; Senda and Nomura, 2003: Yoshukawa et al., 2006). Although presence of HSC has yet to be reported in zebrafish, we found that ATRA-treated zebrafish livers had elevated expression in HSC activation markers (*cryab*b, *spp1 homolog*, *acta2*) (Table 4) (Takahara et al., 2006), which suggest the presence of HSCs and HSCs were activated by ATRA and subsequently modulate hepatocyte morphology (Figure 5, a-d).

Transforming growth factor β (TGF- β) is the major cytokine that promote fibrogenesis in liver fibrosis (Border and Noble, 1994). It has been reported that ATRA initiate TGF- β production in HSCs and aggravate fibrosis (Koda et al., 1996; Okuno et al., 1996; Okuno et al., 2002). Furthermore, retinoids are suggested to potentiate pro-fibrogenic action of TGF-β (Blomhoff, 1997). Thus these studies support the role of ATRA in modulating TGF-β pathway in our experiment (Figure 6). TGF- β has three isoforms, TGF- β1, 2 and

3, and their biological functions are very similar (Border and Noble, 1994). TGF- β1 gene up-regulates in response to hepatic injury the isoform most implicated in fibrosis in organs such as liver, lung and kidney (Border and Noble, 1994). Therefore we verified the elevated expression of transforming growth factor beta 1-like (LOC563884) (Table 4). Thus this suggests the presence of HSCs in zebrafish and also production of TGF- β1 in HSCs by ATRA.

Table 4. *Quantitative real-time PCR validation for selected genes in all-trans retinoic acid treatment.*

		Log2(fold-change) Expression				
		20 nM	200 nM		2000 nM	
Gene Symbol	**Genbank ID**	**Array**	**Array**	**qRT-PCR**	**Array**	**qRT-PCR**
Cytoskeleton						
arpc1a	AI384833	0.09	*0.14	-0.07	**0.09	**0.57
transforming growth factor beta 1-like	LOC563884	NA	NA	*0.96	NA	*0.45
Oxidative stress and its induced responses						
slc25a27	BC053139	-0.24	0.32	*1.05	**0.79	*0.48
cox10	AW342801	0.08	0.16	*0.74	**0.32	**1.30
atp5h	CK400662	0.24	0.34	**0.76	**0.90	**1.91
mlh1	AI558727	0.29	0.19	**1.41	**0.22	**1.54
gclc	AW128066	0.13	0.21	**1.13	*0.30	**0.82
nrf2	CR848724	NA	NA	*1.14	NA	**2.23
psma3	BG306038	0.01	0.1	0.53	**0.29	**1.90
arg2	AW018735	**2.69	0.47	**1.67	**1.94	**0.60
Cell death						
ndrg1	BM185420	0.43	**1.35	**3.11	**1.37	**2.56
casp7	BC095327	0.14	**0.29	**1.36	**0.25	*0.67
casp8	AF273220	0.19	0.3	**0.82	**0.18	**0.87
Protein metabolism						
aco2	BI888674	0.14	*0.25	**1.29	**0.31	**1.74
dlst	BI896563	0.26	**1.89	**0.46	**0.30	**1.22
Immune responses						
jun	BE605692	-0.01	**0.11	**1.32	*0.21	**0.77
fos	BE605310	**0.39	0.24	1.93	**1.04	*1.07
Hepatic stellate cell activation markers						
cryabb	BC076518	0.03	-0.01	**2.93	0.19	*0.63
spp1 homolog	CR925756	NA	NA	**2.45	NA	**1.95
acta2	CU855699	NA	NA	*1.59	NA	*3.23

The genes were selected based on biological function of interest identified by GSEA. The relative $\log_2$ fold-change above controls as determined by quantitative real-time polymerase chain reaction (qRT-PCR) and microarray (Array) are presented (* p-value <0.1; ** p-value < 0.05).

4.2.3 Oxidative phosphorylation & oxidative stress-induced responses

We observed that ATRA treatment increased oxidative phosphorylation and also oxidative stress-induced responses (oxidative stress induced gene expression via nrf2, proteasome, and arginine and proline metabolism) (Figure 6). Several reports had shown that vitamin A and retinoids increased oxidative stress through generation of reactive oxygen species (ROS) which induce cellular damage and death (Davis et al., 1990; Castro-Obregon and Covarrubias, 1996; De Oliveira et al., 2009a; Pasquali et al., 2009). One study showed that ATRA treatment increased mitochondrial electron transfer chain activity in frontal cortex of rat brain (De Oliveira et al., 2009a) and another study demonstrated that ATRA treatment elevated ATP synthesis in mouse liver mitochondria significantly at 2 μM ATRA and higher, which corresponds with the highest concentration used in our experiment and up-regulation in oxidative phosphorylation pathway. We validated increased expression of genes associated with oxidative phosphorylation: solute carrier family 25, member 27 (*slc25a27*), heme A: farnesyltransferase (yeast) (*cox10*) and ATP synthase, H+ transporting, mitochondrial F0 complex, subunit d (*atp5h*). The findings suggest that ATRA elevated oxidative stress in zebrafish liver by increased oxidative phosphorylation. Furthermore, glycogen phosphorylase, the rate limiting enzyme for glycogen degradation, was shown to be carbonylated by oxidative stress in muscles (Fedorova et al., 2010), thus ATRA-induced oxidative stress could inactivate glycogen phosphorylase in zebrafish liver which could lead to increase in hepatic glycogen (Figure 5, i and j).

Nuclear factor erythroid 2-like factor 2 (NRF2), a crucial oxidative-stress inducible transcription factor, has been shown to increase activity and confer mitochondrial protection by inducing expression of cytoprotective and anti-oxidative genes in response to retinoic acid toxicity (Tan et al., 2008). Hence this concurs with the induction of NRF2 pathway (Figure 6) in ATRA treated liver as revealed in our GSEA analysis. This is supported by increased expression in nuclear factor erythroid 2-like factor 2 (*nrf2*) and glutamate-cysteine ligase catalytic subunit (*gclc*), which is a known NRF2's anti-oxidant target gene (Table 4). Moreover, proteasomal degradation was upregulated (Figure 6), and this could be a response to elevated protein damage by oxidative stress. Carbonylation is the most common form of protein modification in response to oxidative stress and this modification is irreversible (Cattaruzza and Hecker, 2008). Protein carbonylation levels was shown to be increased by vitamin A treatment in rat hypothalamus and lungs (De Oliveira et al., 2009b; Pasquali et al., 2009). The up-regulation of arginine and proline metabolism (Figure 6) as revealed in the GSEA analysis could be a result of oxidative carbonylation which is known to preferentially target these amino acids (Cattaruzza and Hecker, 2008). This could be a feedback response to increased oxidative stress-induced removal of carbonylated arginine and proline from damaged proteins. Removal of carbonylated protein is crucial since carbonylated aggregates can become cytotoxic (Nystrom, 2005), thus elevated proteasomal degradation could have inhibited carbonylation-induced cytotoxicity.

4.2.4 Cell death

Our histological analysis showed increased apoptotic activity in the liver parenchyma (Figure 5, g and h), and this is corroborated by up-regulation in pathways associated with apoptosis and mitochondrial-induced apoptosis (Apoptosis KEGG and Role of Mitochondria in Apoptotic Signaling) from our GSEA analysis (Figure 6). This was further validated by the increased gene expression of N-myc downstream regulated gene 1 (*ndrg1*), caspase 7 (*casp7*) and caspase 8 (casp8) which are associated with cell death (Table 4). Up-regulation in Role of Mitochondria in Apoptotic Signaling (Figure 6) suggests that intrinsic apoptosis occurred in the ATRA-treated zebrafish liver ,this is concordant to that which were reported in retinol-treated rat liver mitochondria (Klamt et al., 2005). Klamt et al. (2005) attributed intrinsic apoptosis to retinol-induced mitochondrial oxidative stress. Intrinsic apoptosis may also be triggered by DNA damage, and this is supported by up-regulation of mutL homolog 1, colon cancer, nonpolyposis type 2 (E. coli) (*mlh1*).

4.2.5 Protein and fat metabolism

ATRA treatment down-regulated pathways associated with fatty acid oxidation: mitochondrial fatty acid beta-oxidation, beta-oxidation pathway and fatty acid degradation (Figure 6). There are evidence that showed impaired mitochondrial beta oxidation can contribute to hepatic steatosis (Wei et al., 2008), and therefore down-regulation of fatty acid oxidation could have promoted hepatic steatosis in zebrafish

(Figure 5, k-n). Our result is in agreement with one study that showed ATRA increased hepatic lipid in rats (Çolakoğlu & Kükner, 2003). Other studies have shown retinoids (all-trans-retinoic acid, 13-cis-retinoic acid and natural vitamin A) induced hypertriglyceridemia in rats (Cisneros et al., 2005; Standeven et al., 1996).

Hypertriglyceridemia is shown to be a predictive factor for fatty liver in humans and is closely associated with development of fatty liver (Tsuneto et al., 2010), thus the treatments in earlier studies may have promoted fatty liver, further supporting that retinoids can induce fatty livers and fatty acid metabolism. One study reported that retinoic-induced hypertriglyceridemia is mediated by RAR, since hypertriglyceridemia induced by RAR-selective agonist can be attenuated by co-treatment with RAR-selective antagonist (Standeven et al., 1996). To our knowledge, ATRA-induced suppression of fatty acid oxidation has not been reported. One study showed that elevated angiotensin II in rats induced hepatic mitochondrial oxidative damage which subsequently suppressed mitochondrial fatty acid beta-oxidation and therefore contributed to hepatic steatosis (Osanai and Petkovich, 2005). Another study showed mitochondria to be a susceptible target of ATRA-induced oxidative damage, since knockdown of NRF2, an anti-oxidant transcriptional regulator, exhibited more severe mitochondrial damage (Tan et al., 2008). Therefore hepatic steatosis in zebrafish observed in the histological analysis could be a result of mitochondrial oxidative damage induced by ATRA (Figure 5, k-n). Tricarboxylic acid (TCA) cycle pathway was up-regulated as indicated by GSEA analysis (Figure 6), and was further confirmed elevated expression of associated enzymes determined by quantitative PCR: aconitase 2, mitochondrial (*aco2*) and

dihydrolipoyllysine-residue succinyltransferase component of 2-oxoglutarate dehydrogenase complex, mitochondrial (*dlst*) (Table 4). TCA enzymes were reported to be susceptible targets to carbonylation by reactive oxidative species (Dukan and Nystrom, 1998; Fedorova et al., 2010), and the susceptibility to carbonylation is attributed to either their close proximity to ROS-generating site or its possible physiological role in negative feedback mechanism to control the rate of electron transport chain and ROS production, whereby excessive oxidative stress will deactivate TCA cycle enzymes and subsequently limit the two former respiratory processes (Dukan and Nystrom, 1998).

Thus up-regulation in TCA cycle pathway could be due to oxidative stress-induced carbonylation of TCA cycle enzymes, which consequently elevated transcription of TCA cycle genes to replace damaged enzymes.

4.2.6 Immune responses

ATRA treatment elevated several immune-associated pathways: B cell antigen receptor (BCR) complex pathway, C-C chemokine receptor type 3 signaling pathway and interleukin-2 (IL-2) pathway (Figure 6). The role of ATRA and vitamin A in immune function is well documented whereby vitamin A deficiency impairs immune function (Stephensen, 2001) and ATRA was shown to modulate immune system in rats, thereby magnifying their immune response to lipopolysaccharide in immune system (Seguin-Devaux et al., 2005).

ATRA was shown to enhance hepatic IL2 expression, thus this agrees with increased IL2 signaling pathway in our treatment (Seguin-Devaux et al., 2005). We verified activation of IL2 pathway via validating elevated gene expression of V-jun sarcoma virus 17 oncogene homolog (avian) (*jun*) and V-fos FBJ murine osteosarcoma viral oncogene homolog (*fos*) (Table 4), which are associated with IL2 pathway. High dose ATRA treatment was shown to induce infiltration of inflammatory cells in rat liver (Çolakoğlu & Kükner, 2003), thus this suggest that immune processes and also inflammation may be elevated in zebrafish liver. ATRA treatment has been shown to increase immune cells with in rat blood (Seguin-Devaux et al., 2005), and also specifically B cells in vivo, thus our ATRA-treated liver may have increased number of B cells which could up-regulate B cell antigen receptor (BCR) pathway (Chen et al., 2008). Thus similar ATRA-induced elevated immune processes in zebrafish and mammalian system suggest conservation of response.

4.3 Conserved response between all-trans retinoic acid-treated mouse embryoid bodies and zebrafish

To compare ATRA-induced molecular responses between mammals and zebrafish, we performed a transcriptome meta-analysis of our ATRA-treated zebrafish livers and mouse embryoid bodies (GEO Accession GSE12333, http://www.ncbi.nlm.nih.gov/geo/) that are treated with ATRA using microspheres. The comparative analyses showed that several processes were similarly regulated: fatty acid metabolism, beta-oxidation and mitochondrial fatty acid beta-oxidation pathways were suppressed in zebrafish liver and

mouse embryoid bodies, whereas proteasome pathway was induced (Figure 7). Hence this gives further support that fatty acid oxidation was attenuated in zebrafish liver and could consequently promote hepatic steatosis (Figure 5, k-n). Furthermore, this corroborates up-regulation of proteasome pathway in zebrafish liver which may be due to increased levels of oxidatively damaged proteins. Thus similar suppression in fatty acid oxidation and proteasome degradation suggest conserved ATRA-induced responses in these processes between fish and mammals.

However, there is differential deregulation in TGF-β signaling pathway: it is suppressed in mouse embryoid bodies but elevated in zebrafish liver. ATRA exposure was shown to disrupt TGF- β protein expression in mouse embryonic development, whereby TGF- β1 was reduced in various embryonic tissues and TGF- β2 reduced in all tissues (Mahmood et al., 1992). On contrary, ATRA exposure in mature liver induces TGF- β production (Koda et al., 1996; Okuno et al., 1997; Okuno et al., 2002), thus differential TGF-β response is most likely due to different biological tissues used. This shows conservation in ATRA-induced tissue response between zebrafish and mammals, since zebrafish liver and mammalian liver have induced TGF- β response upon ATRA exposure, unlike embryonic tissues which suppress its expression.

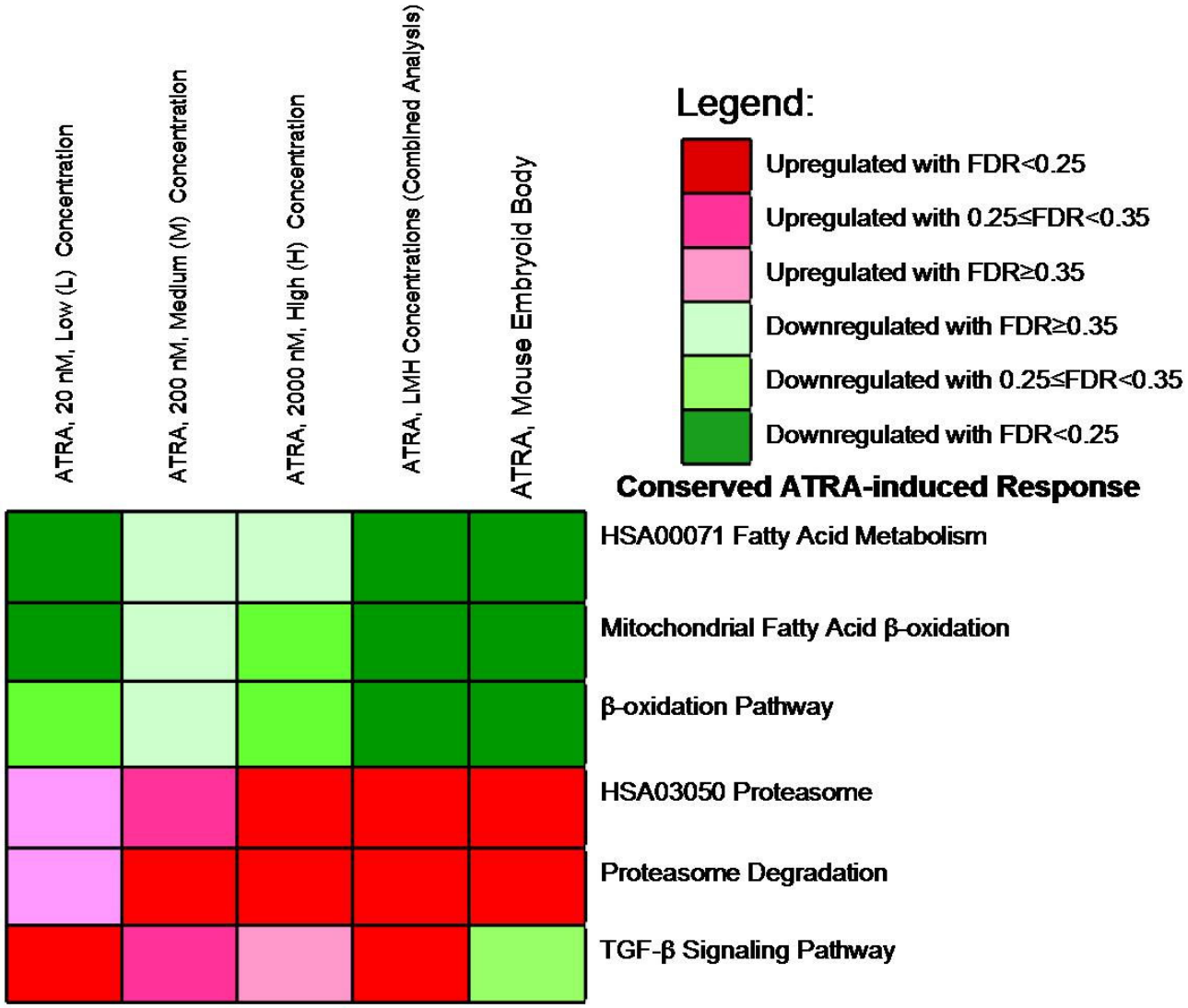

Fig 7. Comparative transcriptome analyses between zebrafish livers and mouse embryoid bodies upon exposure to all-trans retinoic acid (ATRA) using Gene Set Enrichment Analysis (GSEA). GSEA analysis is performed on transcriptome profiles of 20 nM, 200 nM, 2000 nM, all combined three concentrations (20 nM, 200 nM and 2000 nM) of ATRA zebrafish liver-treated groups (LMH) and ATRA-treated mouse embryoid bodies compared to their own respective control groups. Up- and down-regulated gene sets are indicated as different shades of red and green respectively. The shades of red and green are based on the significance of false-discovery rate (FDR) (see figure legend). Biological processes associated with fatty acid β-oxidation (down-regulated) and proteasomal degradation (up-regulated) are similarly dysregulated in ATRA-treated zebrafish livers and mouse embryoid bodies, whereas "TGF-β Signaling Pathway" and "HSA04620 Toll like Receptor Signaling Pathway" are differentially dysregulated in ATRA-treated zebrafish livers (up-regulated) compared to the mouse embryoid bodies (down-regulated).

4.4 Validation of Marker Genes Associated with Canonical Pathways

We confirmed deregulated canonical pathways that were identified from transcriptomic analysis by validating expression levels of relevant genes using real-time PCR in a separate subsequent batch of treated fish under same treatment conditions. Total RNA extracted from the zebrafish livers was reverse-transcribed to cDNA before gene validation using quantitative real-time PCR. We validated 20 genes: actin related protein 2/3 complex, subunit 1A (*arpc1a,* hypothetical protein LOC336379), transforming growth factor beta 1-like (*LOC563884*), protein kinase, solute carrier family 25, member 27 (*slc25a27*), heme A: farnesyltransferase (yeast) (*cox10*), ATP synthase, H+ transporting, mitochondrial F0 complex, subunit d (*atp5h*), mutL homolog 1, colon cancer, nonpolyposis type 2 (E. coli) (*mlh1*), glutamate-cysteine ligase, catalytic subunit (*gclc*), nuclear factor (erythroid-derived 2)-like 2 (*nrf2*), proteasome (prosome, macropain) subunit, alpha type, 3 (*psma3*), arginase, type II (*arg2*), myc downstream regulated gene 1 (*ndrg1*), caspase 7 (*casp7*), caspase 8 (*casp8*), aconitase 2, mitochondrial (*aco2*), dihydrolipoamide S-succinyltransferase (E2 component of 2-oxo-glutarate complex) (*dlst*), v-jun sarcoma virus 17 oncogene homolog (*jun*), V-fos FBJ murine osteosarcoma viral oncogene homolog (*fos*), crystallin, alpha B, b (*cryabb*), secreted phosphoprotein 1 homolog (*spp1 homolog*), actin, alpha 2, smooth muscle, aorta (*acta2*) and cytochrome P450, family 26, subfamily a, polypeptide 1 (*cyp26a1*) (Table 4 and Figure 5f). These genes were significant ($p<0.10$) in at least 2000 nM in arrays and real-time PCR (Table 4 and Figure 5f). These genes confirmed perturbations in several biological processes in the ATRA-treated zebrafish liver: cytoskeleton (*arpc1a,*

LOC336379), oxidative phosphorylation (*slc25a27, cox10, atp5h*), DNA damage repair (*mlh1*), anti-oxidative responses (*nrf2, gclc*), proteasomal degradation (*psma3*), arginine and proline metabolism (*arg2*), p53 signaling pathway (*ndrg1*), caspase pathway (*casp7, casp8*), kreb cycle (*aco2, dlst*), immune response (*jun, fos*), HSC activation markers (*cryabb, spp1 homolog, acta2*), and retinoic acid receptor target gene (*cyp26a1*) (Figure 5f and Table 4). Therefore validation of genes associated with selected biological processes in the repeated batch of ATRA-treated fish, supported our transcriptomic and histological analyses. We showed dose-dependent elevated expression in ATRA target gene cytochrome P450, family 26, subfamily a, polypeptide 1 (*cyp26a1*), a RA-metabolizing enzyme, thus this confirms ATRA-induced responses in zebrafish liver and *cyp26a1*-mediated clearance of RA to attenuate RA signaling (Abu-Abed et al., 2001). *Cyp26a1* could also be induced to abrogate RA-mediated apoptosis through RA clearance (Osanai and Petkovich, 2005).

ATRA-mediated hepatotoxicity was shown to modulate biological processes associated with cytoskeletal assembly and reorganization, oxidative phosphorylation, oxidative stress-induced responses, cellular death and immune response. Modulation in cytoskeletal regulatory pathways (Y branching of actin filaments and TGF-β signaling pathway) were validated by verifying the up-regulation in modulation of actin filaments with the elevated expression of actin related protein 2/3 complex, subunit 1A (*arpc1a,* hypothetical protein LOC336379) and TGF-β (LOC563884). We also verified elevated oxidative stress through oxidative phosphorylation by validating elevated expression of genes associated with oxidative phosphorylation: solute carrier family 25, member 27

(*slc25a27*), heme A: farnesyltransferase (yeast) (*cox10*), ATP synthase, H+ transporting and mitochondrial F0 complex, subunit d (*atp5h*) (Table 3).

Elevated oxidative stress, generated by oxidative phosphorylation, could lead to antioxidant responses, DNA damage, protein damage and cellular apoptosis. We confirmed antioxidant responses through verifying induction of NRF2, an oxidant stress-induced transcriptional regulator, by validating the induction of nuclear factor erythroid 2-like factor 2 (*nrf2*) gene expressions and NRF2's anti-oxidant gene target, glutamate-cysteine ligase catalytic subunit (*gclc*). The inductions of these two genes are concordant with previous study in ATRA-treated rat liver (Tan et al., 2008). Furthermore, we verified DNA damage by validating expression of mutL homolog 1, colon cancer, nonpolyposis type 2 (E. coli) (*mlh1*) (Table 4), which is involved in DNA repair.

Oxidative stress could increase levels of damaged proteins, thus we verified elevated proteasome degradation with proteasome (prosome, macropain) subunit, alpha type, 3 (*psma3*). We also verified upregulation in kreb enzymes, aconitase 2, mitochondrial (*aco2*) and dihydrolipoamide S-succinyltransferase (E2 component of 2-oxo-glutarate complex) (*dlst*), and this could be a response to replace oxidatively damaged enzymes due to elevated oxidative stress. Apoptag staining revealed increased apoptotic activity in the liver parenchyma (Figure 5, g and h), thus we also verified up-regulation in pathways involved in cellular deaths with myc downstream regulated gene 1 (*ndrg1*), caspase 7 (*casp7*) and caspase 8 (*casp8*). Genes associated with immune function was shown to be up-regulated: v-jun sarcoma virus 17 oncogene homolog (*jun*) and V-fos

FBJ murine osteosarcoma viral oncogene homolog (*fos*). Thus this suggests that ATRA induced immune function.

Hypervitaminosis A has been linked closely to HSC activation (Nollevaux et al., 2006). Although presence of HSC has not been reported in zebrafish, we validated the elevated expression of three HSC activation markers (Takahara et al., 2006): crystallin, alpha B, b (*cryabb*), secreted phosphoprotein 1 homolog (*spp1 homolog*), and actin, alpha 2, smooth muscle, aorta *(acta2*). HSC activation is associated with promoting actin remodeling, liver fibrosis and inflammation (Knittel et al., 1999; Reynaert et al., 2008; Brenner, 2009). Trichostatin A (TSA), a histone deactylase inhibitor, was shown to have attenuated fibrogenic action of HSCs (Rombouts et al., 2002). The abrogation of HSC fibrogenic action by TSA was attributed to TSA-induced inhibition in the formation of actin filament via decreasing protein levels of nucleating proteins [actin related protein 2 (Arp2) and Arp3] and therefore attenuate the expression of Arp2/3 complex (Rombouts et al., 2002). Our study suggests that Arp2/3 complex expression is up-regulated since *arpc1a*, a subunit of Arp2/3 complex, was up-regulated (Table 4). Hence this suggests that HSCs are present in zebrafish and its ATRA-induced activation could lead to cytoskeleton remodeling in the liver (Figure 5, a-d) by increased activity of Arp2/3 complex. Furthermore HSC activation could also promote inflammation by attracting inflammatory cells to the injured hepatocytes (Knittel et al., 1999) and subsequently elevated immune-associated pathways (Figure 6). This is concordant to one study that showed increased infiltration in ATRA-treated rat liver (Çolakoğlu & Kükner, 2003).

4.5 Conclusion

This study characterized in vivo mechanistic action of ATRA-induced hepatotoxicity on several important biological processes: cytoskeleton remodeling, oxidative phosphorylation, oxidative stress-induced responses, cell death, protein and fatty acid metabolism, and immune responses. ATRA is a well-characterized agonist ligand for retinoic acid receptor. This is the first report that described in vivo mechanistic action for retinoic acid receptor-mediated hepatoxicity using ATRA, to our knowledge. ATRA-induced molecular responses at systems level are characterized with transcriptome analysis. This analysis was coupled with phenotypic anchoring and selected gene validation to reveal several deregulated biological processes, such as modulating cytoskeleton, oxidative damage, cell death, fatty acid metabolism and immune response, which can cause liver injury. Comparative transcriptome analyses between ATRA-treated zebrafish liver and mouse embryoid bodies revealed some similar conserved molecular responses. Furthermore, we showed that biomarkers for HSC activation were elevated in zebrafish. If HSCs are present in zebrafish, ATRA-induced HSC activation could have promoted cytoskeleton remodeling and inflammation, and consequently contribute to liver damage. Our findings showed that zebrafish system can serve to model ATRA-induced hepatotoxicity in mammals and also for other nuclear receptor-mediated drug action.

Chapter 5
Major conclusions and future directions

5.1 Major conclusions

In this study, we characterized biological responses induced by ligand-activated nuclear receptors, liver X receptors (LXR) and retinoic acid receptors (RAR). LXR and RAR were activated with well-characterized agonists, T0901317 and all-trans retinoic acid (ATRA) respectively. We revealed the responses with transcriptomic analysis, histological examination and validation of gene expression. The major conclusions of this study include the following:

1) We showed that effects induced by activation of RARs and LXR in the zebrafish model are similar to those reported in mammalian models, therefore revealing conserved mode-of-actions between mammals and zebrafish. Furthermore, our study shows that the zebrafish can be used to model hepatotoxicity in mammals and also model nuclear receptor-mediated drug action.

2) In both treatments, we revealed some similar hepatic responses. Histological analysis showed that the hepatocytes membrane became irregular, apoptotic activity and hepatic lipids were elevated. Furthermore, transcriptomic analysis showed that processes associated with cellular structure, fatty acid oxidation and immune function were perturbed.

3a) From transcriptomic analyses, we revealed perturbation of processes associated with cellular morphology and adhesion, coagulation and complement systems, cellular morphology and adhesion, diabetes and beta-oxidation of acids.

3b) Additionally, we identified novel LXR regulated processes. LXR activation was found to transcriptionally repress genes associated with cellular morphology and adhesion, and coagulation and complement systems that could contribute to anti-thrombogenic, anti-atherogenic and anti-inflammatory.

3d) Furthermore, we revealed and validated deregulated genes that are associated with insulin signaling, lipid and gluconeogenesis that could contribute to hepatic steatosis and potentially insulin deficiency.

4a) Transcriptomic analyses revealed that RAR activation perturbed processes associated with cytoskeleton, oxidative phosphorylation and oxidative stress-induced responses, cell death, protein and fat metabolism, and immune responses.

4b) Comparative transcriptomic meta-analyses between ATRA-treated mouse embryoid bodies and zebrafish liver showed similar repression in fatty acid oxidation and up-regulation in proteasomal degradation.

4c) RAR activation induced upregulation in gene markers for hepatic stellate cell (HSC) activation. Furthermore, RAR activation modulates genes associated with cytoskeleton remodeling and inflammatory responses. These responses are associated with HSC activation reported in mammals, thus this suggest that HSCs are present in zebrafish liver, and HSC activation can be studied in zebrafish model.

5.2 Future directions

Biological responses through activation of two nuclear receptors with agonists in zebrafish liver were characterized. Hepatotoxicity was induced in both treatments and metabolic processes were perturbed. The following is an outline of follow-up experiments that can be performed on the basis of present work for both LXR and RAR.

1) Our studies of molecular biological responses were observed at transcriptomic level. Hence it may be interesting to perform proteomics and metabolomics to validate perturbations found at transcriptomic level and also reveal novel perturbations at protein and metabolic level.

2) We can identify suitable gene markers for LXR and RAR activation in zebrafish larvae, using gene markers that were validated in our study with quantitative real-time PCR. These gene markers can be used in future for high-throughput gene-expression-based screens with zebrafish larvae for LXR and RAR disruptors.

In addition, the following can be considered for LXR and RAR separately.

A. Liver X receptor

1) There are other LXR agonists available, hence comparative transcriptome analysis with GW3965 can be performed to find any differing gene induction. Differing responses allow us to identify responses that are not LXR-mediated.

2) Developmental screens in zebrafish embryos for LXR perturbation has yet to be characterized, hence LXR-induced developmental perturbations can be characterized. This can facilitate future phenotype-based screens for LXR perturbations.

3) Identify LXR agonists' off-target toxicity effects in zebrafish embryos. We can reveal off-target effects by comparing differing developmental defects between elevated expression of LXR mRNA (via transgenic induction or injection of LXR mRNA) to treatment with LXR agonists.

4) LXR has been proposed as a target for diabetic treatment; however whether LXR induction promotes insulin deficiency is unclear. Hence we can perform LXR activation in zebrafish through chronic exposure to LXR agonist or develop transgenic lines that induce LXR levels in liver and/or pancreas. Acute LXR agonist treatment can be performed in transgenic fluorescent reporter lines for liver and pancreas in zebrafish larvae to visualize toxicological perturbations in these organs.

B. Retinoic acid receptor

1) Validate the presence of HSC in zebrafish. HSC promotes liver fibrosis during its active state; however its role in quiescent state is unclear. Development of transgenic zebrafish to study the role of HSCs can reveal its function during quiescent state and also validate ATRA induces HSC activation. For example, transgenic zebrafish that allows specific obliteration of HSC to allow how deficiency of HSCs can affect liver function. Additionally, transgenic fluorescent reporter lines for HSCs in zebrafish can be created to allow in vivo confocal imaging in larvae; this facilitates observation of changes in HSC after ATRA or other chemical treatment.

2) Study effects of chronic exposure to ATRA in adult zebrafish liver, since current study involves acute exposure. Chronic exposure will more closely resemble hypervitaminosis A condition in humans and have more relevance in investigating its health effects.

3) Characterize RAR-mediated perturbation in further detail. Perform transcriptomic studies with RAR antagonist and make comparative analyses with ATRA treatment.

References

Abu-Abed S, Dolle P, Metzger D, Beckett B, Chambon P, and Petkovich M. The retinoic acid-metabolizing enzyme, CYP26A1, is essential for normal hindbrain patterning, vertebral identity, and development of posterior structures, 2001. Genes Dev 15:226-240.

Allen LH, and Haskell M. Estimating the potential for vitamin A toxicity in women and young children, 2002. J Nutr 132:2907S-2919S.

Amara U, Rittirsch D, Flierl M, Bruckner U, Klos A, Gebhard F, Lambris JD, and Huber-Lang M. Interaction between the coagulation and complement system, 2008. Adv Exp Med Biol 632:71-79.

Archer A, Lauter G, Hauptmann G, Mode A, and Gustafsson JA. Transcriptional activity and developmental expression of liver X receptor (lxr) in zebrafish, 2008. Dev Dyn 237:1090-1098.

Baker AH, Edwards DR, and Murphy G. Metalloproteinase inhibitors: biological actions and therapeutic opportunities, 2002. J Cell Sci 115:3719-3727.

Baranowski M. Biological role of liver X receptors, 2008. J Physiol Pharmacol 59 Suppl 7:31-55.

Basciano H, Miller A, Baker C, Naples M, and Adeli K. LXRalpha activation perturbs hepatic insulin signaling and stimulates production of apolipoprotein B-containing lipoproteins, 2009. Am J Physiol Gastrointest Liver Physiol 297:G323-332.

Blaschke F, Takata Y, Caglayan E, Collins A, Tontonoz P, Hsueh WA, and Tangirala RK. A nuclear receptor corepressor-dependent pathway mediates suppression of cytokine-induced C-reactive protein gene expression by liver X receptor, 2006. Circ Res 99:e88-99.

Blomhoff R. Retinoids may increase fibrotic potential of TGF-beta: crosstalk between two multi-functional effectors, 1997. Hepatology 26:1067-1068.

Blomhoff R, and Wake K. Perisinusoidal stellate cells of the liver: important roles in retinol metabolism and fibrosis, 1991. Faseb J 5:271-277.

Blomme EA, Yang Y, and Waring JF. Use of toxicogenomics to understand mechanisms of drug-induced hepatotoxicity during drug discovery and development, 2009. Toxicol Lett 186:22-31.

Border WA, and Noble NA. Transforming growth factor beta in tissue fibrosis, 1994. N Engl J Med 331:1286-1292.

Brenner DA. Molecular pathogenesis of liver fibrosis, 2009. Trans Am Clin Climatol Assoc 120:361-368.

Butcher EC, Berg EL, and Kunkel EJ. Systems biology in drug discovery, 2004. Nat Biotechnol 22:1253-1259.

Camerer E, Kolsto AB, and Prydz H. Cell biology of tissue factor, the principal initiator of blood coagulation, 1996. Thromb Res 81:1-41.

Cao G, Liang Y, Broderick CL, Oldham BA, Beyer TP, Schmidt RJ, Zhang Y, Stayrook KR, Suen C, Otto KA, Miller AR, Dai J, Foxworthy P, Gao H, Ryan TP, Jiang XC, Burris TP, Eacho PI, and Etgen GJ. Antidiabetic action of a liver x receptor agonist mediated by inhibition of hepatic gluconeogenesis, 2003. J Biol Chem 278:1131-1136.

Castrillo A, Joseph SB, Marathe C, Mangelsdorf DJ, and Tontonoz P. Liver X receptor-dependent repression of matrix metalloproteinase-9 expression in macrophages, 2003. J Biol Chem 278:10443-10449.

Castro-Obregon S, and Covarrubias L. Role of retinoic acid and oxidative stress in embryonic stem cell death and neuronal differentiation, 1996. FEBS Lett 381:93-97.

Cattaruzza M, and Hecker M. Protein carbonylation and decarboylation: a new twist to the complex response of vascular cells to oxidative stress, 2008. Circ Res 102:273-274.

Chapin, RE, Adams J, Boekelheide K, Gray LE, Hayward SW Jr, Lees PS, McIntyre BS, Portier KM, Schnorr TM, Selevan SG, Vandenbergh JG, and Woskie SR. NTP-CERHR expert panel report on the reproductive and developmental toxicity of bisphenol A, 2008. Birth Defects Res B Dev Reprod Toxicol 83:157-395.

Chen X, Esplin BL, Garrett KP, Welner RS, Webb CF, and Kincade PW. Retinoids accelerate B lineage lymphoid differentiation, 2008. J Immunol 180:138-145.

Cheng O, Ostrowski RP, Liu W, and Zhang JH. Activation of liver X receptor reduces global ischemic brain injury by reduction of nuclear factor-kappaB, 2010. Neuroscience 166:1101-1109.

Chintalacharuvu SR, Sandusky GE, Burris TP, Burmer GC, and Nagpal S. Liver X receptor is a therapeutic target in collagen-induced arthritis, 2007. Arthritis Rheum 56:1365-1367.

Chisholm JW, Hong J, Mills SA, and Lawn RM. The LXR ligand T0901317 induces severe lipogenesis in the db/db diabetic mouse, 2003. J Lipid Res 44:2039-2048.

Choe SS, Choi AH, Lee JW, Kim KH, Chung JJ, Park J, Lee KM, Park KG, Lee IK, and Kim JB. Chronic activation of liver X receptor induces beta-cell apoptosis through

hyperactivation of lipogenesis: liver X receptor-mediated lipotoxicity in pancreatic beta-cells, 2007. Diabetes 56:1534-1543.

Cisneros FJ, Gough BJ, Patton RE, and Ferguson SA. Serum levels of albumin, triglycerides, total protein and glucose in rats are altered after oral treatment with low doses of 13-cis-retinoic acid or all-trans-retinoic acid, 2005. J Appl Toxicol 25:470-478.

Çolakoglu N, and Kükner A. Effects of high dose retinoic acid on adult rat liver: electron microscopic and immunohistochemical study, 2003. 23, 4, p. 509-517.

Collins JL, Fivush AM, Watson MA, Galardi CM, Lewis MC, Moore LB, Parks DJ, Wilson JG, Tippin TK, Binz JG, Plunket KD, Morgan DG, Beaudet EJ, Whitney KD, Kliewer SA, and Willson TM. Identification of a nonsteroidal liver X receptor agonist through parallel array synthesis of tertiary amines, 2002. J Med Chem 45:1963-1966.

Davis WL, Crawford LA, Cooper OJ, Farmer GR, Thomas D, and Freeman BL. Generation of radical oxygen species by neural crest cells treated in vitro with isotretinoin and 4-oxo-isotretinoin, 1990. J Craniofac Genet Dev Biol 10:295-310.

De Oliveira MR, Oliveira MW, Behr GA, and Moreira JC. Vitamin A supplementation at clinical doses induces a dysfunction in the redox and bioenergetics states, but did change neither caspases activities nor TNF-alpha levels in the frontal cortex of adult Wistar rats, 2009a. J Psychiatr Res 43:754-762.

De Oliveira MR, Oliveira MW, Da Rocha RF, and Moreira JC. Vitamin A supplementation at pharmacological doses induces nitrosative stress on the hypothalamus of adult Wistar rats, 2009b. Chem Biol Interact 180:407-413.

Detrich HW 3rd, Westerfield M, and Zon LI. Overview of the Zebrafish system, 1999. Methods Cell Biol 59:3-10.

Dukan S, and Nystrom T. Bacterial senescence: stasis results in increased and differential oxidation of cytoplasmic proteins leading to developmental induction of the heat shock regulon, 1998. Genes Dev 12:3431-3441.

Fawcett J, and Duckworth WC. Hyperglycaemia and hyperinsulinaemia: is insulin-degrading enzyme the missing link? 2009. Diabetologia 52:1457-1460.

Fawcett J, Hamel FG, Duckworth WC. Characterization of the inhibition of protein degradation by insulin in L6 cells. Arch Biochem Biophys. 2001 Jan 15;385(2):357-63.

Fedorova M, Kuleva N, and Hoffmann R. Identification, quantification, and functional aspects of skeletal muscle protein-carbonylation in vivo during acute oxidative stress, 2010. J Proteome Res 9:2516-2526.

Ganter B, Tugendreich S, Pearson CI, Ayanoglu E, Baumhueter S, Bostian KA, Brady L, Browne LJ, Calvin JT, Day GJ, Breckenridge N, Dunlea S, Eynon BP, Furness LM, Ferng J, Fielden MR, Fujimoto SY, Gong L, Hu C, Idury R, Judo MS, Kolaja KL, Lee MD, McSorley C, Minor JM, Nair RV, Natsoulis G, Nguyen P, Nicholson SM, Pham H, Roter AH, Sun D, Tan S, Thode S, Tolley AM, Vladimirova A, Yang J, Zhou Z, and Jarnagin K. Development of a large-scale chemogenomics database to improve drug candidate selection and to understand mechanisms of chemical toxicity and action, 2005. J Biotechnol 119:219-244.

Ghisletti S, Huang W, Jepsen K, Benner C, Hardiman G, Rosenfeld MG, and Glass CK. Cooperative NCoR/SMRT interactions establish a corepressor-based strategy for integration of inflammatory and anti-inflammatory signaling pathways, 2009. Genes Dev 23:681-693.

Glass CK, and Witztum JL. Atherosclerosis. the road ahead, 2001. Cell 104:503-516.

Grefhorst A, van Dijk TH, Hammer A, van der Sluijs FH, Havinga R, Havekes LM, Romijn JA, Groot PH, Reijngoud DJ, and Kuipers F. Differential effects of pharmacological liver X receptor activation on hepatic and peripheral insulin sensitivity in lean and ob/ob mice, 2005. Am J Physiol Endocrinol Metab 289:E829-838.

Grun, F, and Blumberg B. Environmental obesogens: organotins and endocrine disruption via nuclear receptor signaling, 2006. Endocrinology 147:S50-55.

Gurvich, N, Berman MG, Wittner BS, Gentleman RC, Klein PS, and Green JB. Association of valproate-induced teratogenesis with histone deacetylase inhibition in vivo, 2005. Faseb J 19:1166-1168.

Hale LA, Tallafuss A, Yan YL, Dudley L, Eisen JS, and Postlethwait JH. Characterization of the retinoic acid receptor genes raraa, rarab and rarg during zebrafish development, 2006. Gene Expr Patterns 6:546-555.

Hans S, and Westerfield M. Changes in retinoic acid signaling alter otic patterning, 2007. Development 134:2449-2458.

Harrill AH, and Rusyn I. Systems biology and functional genomics approaches for the identification of cellular responses to drug toxicity, 2008. Expert Opin Drug Metab Toxicol 4:1379-1389.

Hegedus Z, Zakrzewska A, Agoston VC, Ordas A, Racz P, Mink M, Spaink HP, and Meijer AH. Deep sequencing of the zebrafish transcriptome response to mycobacterium infection, 2009. Mol Immunol 46:2918-2930.

Hieronymus H, Lamb J, Ross KN, Peng XP, Clement C, Rodina A, Nieto M, Du J, Stegmaier K, Raj SM, Maloney KN, Clardy J, Hahn WC, Chiosis G, and Golub TR.

Gene expression signature-based chemical genomic prediction identifies a novel class of HSP90 pathway modulators, 2006. Cancer Cell 10:321-330.

Hill AJ, Teraoka H, Heideman W, and Peterson RE. Zebrafish as a model vertebrate for investigating chemical toxicity, 2005. Toxicol Sci 86:6-19.

Hiltona JW, Choa CY, and Slingera SJ. Effect of hypervitaminosis A on the development of ascorbic acid deficiency in underyearling rainbow trout (Salmo gairdneri), 1978. Aquaculture 13:325-330.

Hutton JC, and O'Brien RM. Glucose-6-phosphatase catalytic subunit gene family, 2009. J Biol Chem 284:29241-29245.

Jakobsson T, Osman WO, Gustafsson JA, Zilliacus J, and Warnmark A. Molecular basis for repression of liver X receptor-mediated gene transcription by receptor-interacting protein 140, 2007. Biochem J 405:31-39.

Joseph SB, Castrillo A, Laffitte BA, Mangelsdorf DJ, and Tontonoz P. Reciprocal regulation of inflammation and lipid metabolism by liver X receptors, 2003. Nat Med 9:213-219.

Joseph SB, McKilligin E, Pei L, Watson MA, Collins AR, Laffitte BA, Chen M, Noh G, Goodman J, Hagger GN, Tran J, Tippin TK, Wang X, Lusis AJ, Hsueh WA, Law RE, Collins JL, Willson TM, and Tontonoz P. Synthetic LXR ligand inhibits the development of atherosclerosis in mice, 2002. Proc Natl Acad Sci U S A 99:7604-7609.

Kane MA, Folias AE, Wang C, and Napoli JL. Quantitative profiling of endogenous retinoic acid in vivo and in vitro by tandem mass spectrometry, 2008. Anal Chem 80:1702-1708.

Klamt F, Roberto de Oliveira M, and Moreira JC. Retinol induces permeability transition and cytochrome c release from rat liver mitochondria, 2005. Biochim Biophys Acta 1726:14-20.

Knittel T, Dinter C, Kobold D, Neubauer K, Mehde M, Eichhorst S, and Ramadori G. Expression and regulation of cell adhesion molecules by hepatic stellate cells (HSC) of rat liver: involvement of HSC in recruitment of inflammatory cells during hepatic tissue repair, 1999. Am J Pathol 154:153-167.

Koda H, Okuno M, Imai S, Moriwaki H, Muto Y, Kawada N, and Kojima S. Retinoic acid-stimulated liver stellate cells suppress the production of albumin from parenchymal cells via TGF-beta, 1996. Biochem Biophys Res Commun 221:565-569.

Korbelik M. Complement upregulation in photodynamic therapy-treated tumors: Role of Toll-like receptor pathway and NFkappaB, 2009. Cancer Lett 281:232-238.

Kotokorpi P, Gardmo C, Nystrom CS, and Mode A. Activation of the glucocorticoid receptor or liver X receptors interferes with growth hormone-induced akr1b7 gene expression in rat hepatocytes, 2004. Endocrinology 145:5704-5713.

Laale H. The biology and use of zebrafish, Brachydanio rerio in fisheries research, 1997. Journal of Fish Biology. 10:121-173.

Lam SH, Winata CL, Tong Y, Korzh S, Lim WS, Korzh V, Spitsbergen J, Mathavan S, Miller LD, Liu ET, and Gong Z. Transcriptome kinetics of arsenic-induced adaptive response in zebrafish liver, 2006a. Physiol Genomics 27:351-361.

Lam SH, Krishna Murthy Karuturi R, and Gong Z. Zebrafish spotted-microarray for genome-wide expression profiling experiments: data acquisition and analysis, 2009a. Methods Mol Biol 546:197-226.

Lam, SH, Mathavan S, and Gong Z. Zebrafish spotted-microarray for genome-wide expression profiling experiments. Part I: array printing and hybridization, 2009b. Methods Mol Biol 546:175-195.

Lam SH, Mathavan S, Tong Y, Li H, Karuturi RK, Wu Y, Vega VB, Liu ET, and Gong Z. Zebrafish whole-adult-organism chemogenomics for large-scale predictive and discovery chemical biology, 2008. PLoS Genet 4:e1000121.

Lam SH, Wu YL, Vega VB, Miller LD, Spitsbergen J, Tong Y, Zhan H, Govindarajan KR, Lee S, Mathavan S, Murthy KR, Buhler DR, Liu ET, and Gong Z. Conservation of gene expression signatures between zebrafish and human liver tumors and tumor progression, 2006b. Nat Biotechnol 24:73-75.

Lamb J, Crawford ED, Peck D, Modell JW, Blat IC, Wrobel MJ, Lerner J, Brunet JP, Subramanian A, Ross KN, Reich M, Hieronymus H, Wei G, Armstrong SA, Haggarty SJ, Clemons PA, Wei R, Carr SA, Lander ES, and Golub TR. The Connectivity Map: using gene-expression signatures to connect small molecules, genes, and disease, 2006. Science 313:1929-1935.

Lecker SH, Solomon V, Price SR, Kwon YT, Mitch WE, Goldberg AL. Ubiquitin conjugation by the N-end rule pathway and mRNAs for its components increase in muscles of diabetic rats. J Clin Invest. 1999 Nov;104:1411-20.

Lefebvre P, Martin PJ, Flajollet S, Dedieu S, Billaut X, and Lefebvre B. Transcriptional activities of retinoic acid receptors, 2005. Vitam Horm 70:199-264.

Li N, Rivera-Bermudez MA, Zhang M, Tejada J, Glasson SS, Collins-Racie LA, Lavallie ER, Wang Y, Chang KC, Nagpal S, Morris EA, Flannery CR, and Yang Z. LXR modulation blocks prostaglandin E2 production and matrix degradation in cartilage and alleviates pain in a rat osteoarthritis model, 2010a. Proc Natl Acad Sci U S A.

Li X, Yeh V, and Molteni V. Liver X receptor modulators: a review of recently patented compounds (2007 - 2009), 2010b. Expert Opin Ther Pat 20:535-562.

Lieschke GJ, and Currie PD. Animal models of human disease: zebrafish swim into view, 2007. Nat Rev Genet 8:353-367.

Lusis AJ. Atherosclerosis, 2000. Nature 407:233-241.

Mackman N. Regulation of the tissue factor gene, 1997. Thromb Haemost 78:747-754.

Maglich JM, Caravella JA, Lambert MH, Willson TM, Moore JT, and Ramamurthy L. The first completed genome sequence from a teleost fish (Fugu rubripes) adds significant diversity to the nuclear receptor superfamily, 2003. Nucleic Acids Res 31:4051-4058.

Mahmood R, Flanders KC, and Morriss-Kay GM. Interactions between retinoids and TGF beta s in mouse morphogenesis, 1992. Development 115:67-74.

Markiewski MM, Nilsson B, Ekdahl KN, Mollnes TE, and Lambris JD. Complement and coagulation: strangers or partners in crime? 2007. Trends Immunol 28:184-192.

Mason DP, Kenagy RD, Hasenstab D, Bowen-Pope DF, Seifert RA, Coats S, Hawkins SM, and Clowes AW. Matrix metalloproteinase-9 overexpression enhances vascular smooth muscle cell migration and alters remodeling in the injured rat carotid artery, 1999. Circ Res 85:1179-1185.

Mattingly CJ, Hampton TH, Brothers KM, Griffin NE, and Planchart A. Perturbation of defense pathways by low-dose arsenic exposure in zebrafish embryos, 2009. Environ Health Perspect 117:981-987.

Meijer AH, Verbeek FJ, Salas-Vidal E, Corredor-Adamez M, Bussman J, van der Sar AM, Otto GW, Geisler R, and Spaink HP. Transcriptome profiling of adult zebrafish at the late stage of chronic tuberculosis due to Mycobacterium marinum infection, 2005. Mol Immunol 42:1185-1203.

Moggs JG, Tinwell H, Spurway T, Chang HS, Pate I, Lim FL, Moore DJ, Soames A, Stuckey R, Currie R, Zhu T, Kimber I, Ashby J, and Orphanides G. Phenotypic anchoring of gene expression changes during estrogen-induced uterine growth, 2004. Environ Health Perspect 112:1589-1606.

Nadauld LD, Shelton DN, Chidester S, Yost HJ, and Jones DA. The zebrafish retinol dehydrogenase, rdh1l, is essential for intestinal development and is regulated by the tumor suppressor adenomatous polyposis coli, 2005. J Biol Chem 280:30490-30495.

Ng AN, de Jong-Curtain TA, Mawdsley DJ, White SJ, Shin J, Appel B, Dong PD, Stainier DY, and Heath JK. Formation of the digestive system in zebrafish: III. Intestinal epithelium morphogenesis, 2005. Dev Biol 286:114-135.

Niculescu F, and Rus H. Complement activation and atherosclerosis, 1999. Mol Immunol 36:949-955.

Nollevaux MC, Guiot Y, Horsmans Y, Leclercq I, Rahier J, Geubel AP, and Sempoux C. Hypervitaminosis A-induced liver fibrosis: stellate cell activation and daily dose consumption, 2006. Liver Int 26:182-186.

Nystrom T. Role of oxidative carbonylation in protein quality control and senescence, 2005. Embo J 24:1311-1317.

Ogata H, and Oku H. The effects of dietary retinoic acid on body lipid deposition in juvenile red sea bream (Pagrus major); a preliminary study, 2001. 193, 3-4, p. 271-279.

Okroj M, Heinegard D, Holmdahl R, and Blom AM. Rheumatoid arthritis and the complement system, 2007. Ann Med 39:517-530.

Okuno M, Moriwaki H, Imai S, Muto Y, Kawada N, Suzuki Y, and Kojima S. Retinoids exacerbate rat liver fibrosis by inducing the activation of latent TGF-beta in liver stellate cells, 1997. Hepatology 26:913-921.

Okuno M, Kojima S, Akita K, Matsushima-Nishiwaki R, Adachi S, Sano T, Takano Y, Takai K, Obora A, Yasuda I, Shiratori Y, Okano Y, Shimada J, Suzuki Y, Muto Y, and Moriwaki Y. Retinoids in liver fibrosis and cancer, 2002. Front Biosci 7:d204-218.

Osanai M, and Petkovich M. Expression of the retinoic acid-metabolizing enzyme CYP26A1 limits programmed cell death, 2005. Mol Pharmacol 67:1808-1817.

Parng C, Seng WL, Semino C, and McGrath P. Zebrafish: a preclinical model for drug screening, 2002. Assay Drug Dev Technol 1:41-48.

Pasquali MA, Gelain DP, de Oliveira MR, Behr GA, da Motta LL, da Rocha RF, Klamt F, and Moreira JC. Vitamin A supplementation for different periods alters oxidative parameters in lungs of rats, 2009. J Med Food 12:1375-1380.

Paules R. Phenotypic anchoring: linking cause and effect, 2003. Environ Health Perspect 111:A338-339.

Peerschke EI, Yin W, Ghebrehiwet B. Complement activation on platelets: implications for vascular inflammation and thrombosis. Mol Immunol. 2010 Aug;47:2170-5.

Penniston KL, and Tanumihardjo SA. The acute and chronic toxic effects of vitamin A, 2006. Am J Clin Nutr 83:191-201.

Peterson RT, Shaw SY, Peterson TA, Milan DJ, Zhong TP, Schreiber SL, C. MacRae A, and Fishman MC. Chemical suppression of a genetic mutation in a zebrafish model of aortic coarctation, 2004. Nat Biotechnol 22:595-599.

Piao YF, Shi Y, and Gao PJ. Inhibitory effect of all-trans retinoic acid on human hepatocellular carcinoma cell proliferation, 2003. World J Gastroenterol 9:2117-2120.

Pommier AJ, Alves G, Viennois E, Bernard S, Y. Communal SY, Sion B, Marceau G, Damon C, Mouzat K, Caira F, Baron S, and Lobaccaro JM. Liver X Receptor activation downregulates AKT survival signaling in lipid rafts and induces apoptosis of prostate cancer cells, 2006. Oncogene 29:2712-2723.

Prescott MF, Sawyer WK, Von Linden-Reed J, Jeune M, Chou M, Caplan SL, and Jeng AY. Effect of matrix metalloproteinase inhibition on progression of atherosclerosis and aneurysm in LDL receptor-deficient mice overexpressing MMP-3, MMP-12, and MMP-13 and on restenosis in rats after balloon injury, 1999. Ann N Y Acad Sci 878:179-190.

Repa, JJ, and Mangelsdorf DJ. The liver X receptor gene team: potential new players in atherosclerosis, 2002. Nat Med 8:1243-1248.

Repa JJ, Turley SD, Lobaccaro JA, Medina J, Li L, Lustig K, Shan B, Heyman RA, Dietschy JM, and Mangelsdorf DJ. Regulation of absorption and ABC1-mediated efflux of cholesterol by RXR heterodimers, 2000. Science 289:1524-1529.

Reynaert H, Urbain D, and Geerts A. Regulation of sinusoidal perfusion in portal hypertension, 2008. Anat Rec (Hoboken) 291:693-698.

Rooyackers OE, Nair KS. Hormonal regulation of human muscle protein metabolism. Annu Rev Nutr. 1997;17:457-85.

Rombouts K, Knittel T, Machesky L, Braet F, Wielant A, Hellemans K, De Bleser P, Gelman I, Ramadori G, and Geerts A. Actin filament formation, reorganization and migration are impaired in hepatic stellate cells under influence of trichostatin A, a histone deacetylase inhibitor, 2002. J Hepatol 37:788-796.

Rough JJ, Monroy MA, Yerrum S, and Daly JM. Anti-proliferative effect of LXR agonist T0901317 in ovarian carcinoma cells, 2010. J Ovarian Res 3:13.

Russell DW. Nuclear orphan receptors control cholesterol catabolism, 1999. Cell 97:539-542.

Schlegel A, and Stainier DY. Lessons from "lower" organisms: what worms, flies, and zebrafish can teach us about human energy metabolism, 2007. PLoS Genet 3:e199.

Scholz H, Lund T, Dahle MK, Collins JL, Korsgren O, Wang JE, and Foss A. The synthetic liver X receptor agonist GW3965 reduces tissue factor production and inflammatory responses in human islets in vitro, 2009. Diabetologia 52:1352-1362.

Seguin-Devaux C, Hanriot D, Dailloux M, Latger-Cannard V, Zannad F, Mertes PM, Longrois D, and Devaux Y. Retinoic acid amplifies the host immune response to LPS through increased T lymphocytes number and LPS binding protein expression, 2005. Mol Cell Endocrinol 245:67-76.

Senda T, and Nomura R. The expression of cytokeratin in hepatic stellate cells of the cod, 2003. Arch Histol Cytol 66:437-444.

Simmonds RE, and Foxwell BM. Signalling, inflammation and arthritis: NF-kappaB and its relevance to arthritis and inflammation, 2008. Rheumatology (Oxford) 47:584-590.

Singh M, and Singh VN. Fatty liver in hypervitaminosis A: synthesis and release of hepatic triglycerides, 1978. Am J Physiol 234:E511-514.

Standeven AM, Beard RL, Johnson AT, Boehm MF, Escobar M, Heyman RA, and Chandraratna RA. Retinoid-induced hypertriglyceridemia in rats is mediated by retinoic acid receptors, 1996. Fundam Appl Toxicol 33:264-271.

Steffensen KR, and Gustafsson JA. Putative metabolic effects of the liver X receptor (LXR), 2004. Diabetes 53 Suppl 1:S36-42.

Stephensen CB. Vitamin A, infection, and immune function, 2001. Annu Rev Nutr 21:167-192.

Stern HM, and Zon LI. Cancer genetics and drug discovery in the zebrafish, 2003. Nat Rev Cancer 3:533-539.

Streisinger G, Walker C, Dower N, Knauber D, and Singer F. Production of clones of homozygous diploid zebra fish (Brachydanio rerio), 1981. Nature 291:293-296.

Subramanian A, Tamayo P, Mootha VK, Mukherjee S, Ebert BL, Gillette MA, Paulovich A, Pomeroy SL, Golub TR, Lander ES, and Mesirov JP. Gene set enrichment analysis: a knowledge-based approach for interpreting genome-wide expression profiles, 2005. Proc Natl Acad Sci U S A 102:15545-15550.

Sullivan C, and Kim CH. Zebrafish as a model for infectious disease and immune function, 2008. Fish Shellfish Immunol 25:341-350.

Takahara Y, Takahashi M, Wagatsuma H, Yokoya F, Zhang QW, Yamaguchi M, Aburatani H, and Kawada N. Gene expression profiles of hepatic cell-type specific marker genes in progression of liver fibrosis, 2006. World J Gastroenterol 12:6473-6499.

Tan KP, Kosuge K, Yang M, and Ito S. NRF2 as a determinant of cellular resistance in retinoic acid cytotoxicity, 2008. Free Radic Biol Med 45:1663-1673.

Tang GW, and Russell RM. 13-cis-retinoic acid is an endogenous compound in human serum, 1990. J Lipid Res 31:175-182.

Terasaka N, Hiroshima A, Ariga A, Honzumi S, Koieyama T, Inaba T, and Fujiwara T. Liver X receptor agonists inhibit tissue factor expression in macrophages, 2005. Febs J 272:1546-1556.

Tiefenbach J, Moll PR, Nelson MR, Hu C, Baev L, Kislinger T, and Krause HM. A live zebrafish-based screening system for human nuclear receptor ligand and cofactor discovery, 2010. PLoS One 5:e9797.

Tilton F, Tilton SC, Bammler TK, Beyer R, Farin F, Stapleton PL, and Gallagher EP. Transcriptional biomarkers and mechanisms of copper-induced olfactory injury in zebrafish, 2008. Environ Sci Technol 42:9404-9411.

Tobin JF, and Freedman LP. Nuclear receptors as drug targets in metabolic diseases: new approaches to therapy, 2006. Trends Endocrinol Metab 17:284-290.

Tsuneto A, Hida A, Sera N, Imaizumi M, Ichimaru S, Nakashima E, Seto S, Maemura K, and Akahoshi M. Fatty liver incidence and predictive variables, 2010. Hypertens Res 33:638-643.

Ung CY, Lam SH, Hlaing MM, Winata CL, Korzh S, Mathavan S, and Gong Z. Mercury-induced hepatotoxicity in zebrafish: in vivo mechanistic insights from transcriptome analysis, phenotype anchoring and targeted gene expression validation, 2010. BMC Genomics 11:212.

van Boxtel AL, Kamstra JH, Cenijn PH, Pieterse B, Wagner JM, Antink M, Krab K, van der Burg B, Marsh G, Brouwer A, and Legler J. Microarray analysis reveals a mechanism of phenolic polybrominated diphenylether toxicity in zebrafish, 2008. Environ Sci Technol 42:1773-1779.

Van der Heiden K, Cuhlmann S, Luong le A, Zakkar M, and Evans PC. Role of nuclear factor kappaB in cardiovascular health and disease, 2010. Clin Sci (Lond) 118:593-605.

van der Ven K, Keil D, Moens LN, Hummelen PV, van Remortel P, Maras M, and De Coen W. Effects of the antidepressant mianserin in zebrafish: molecular markers of endocrine disruption, 2006. Chemosphere 65:1836-1845.

van Vliet T, Boelsma E, de Vries AJ, and van den Berg H. Retinoic acid metabolites in plasma are higher after intake of liver paste compared with a vitamin A supplement in women, 2001. J Nutr 131:3197-3203.

Verschuren L, de Vries-van der Weij J, Zadelaar S, Kleemann R, and Kooistra T. LXR agonist suppresses atherosclerotic lesion growth and promotes lesion regression in apoE*3Leiden mice: time course and mechanisms, 2009. J Lipid Res 50:301-311.

Villeneuve L, Wang RL, Bencic DC, Biales AD, Martinovic D, Lazorchak JM, Toth G, and Ankley GT. Altered gene expression in the brain and ovaries of zebrafish (Danio rerio) exposed to the aromatase inhibitor fadrozole: microarray analysis and hypothesis generation, 2009. Environ Toxicol Chem 28:1767-1782.

Wang Z, Gerstein M, and Snyder M. RNA-Seq: a revolutionary tool for transcriptomics, 2009. Nat Rev Genet 10:57-63.

Waxman JS, and Yelon D. Comparison of the expression patterns of newly identified zebrafish retinoic acid and retinoid X receptors, 2007. Dev Dyn 236:587-595.

Webb KJ, Norton WH, Trumbach D, Meijer AH, Ninkovic J, Topp S, Heck D, Marr C, Wurst W, Theis FJ, Spaink HP, and Bally-Cuif L. Zebrafish reward mutants reveal novel transcripts mediating the behavioral effects of amphetamine, 2009. Genome Biol 10:R81.

Wei Y, Rector RS, Thyfault JP, and Ibdah JA. Nonalcoholic fatty liver disease and mitochondrial dysfunction, 2008. World J Gastroenterol 14:193-199.

Wilhelm BT, and Landry JR. RNA-Seq-quantitative measurement of expression through massively parallel RNA-sequencing, 2009. Methods 48:249-257.

Wu, S, Yin R, Ernest R, Li Y, Zhelyabovska O, Luo J, Yang Y, and Yang Q. Liver X receptors are negative regulators of cardiac hypertrophy via suppressing NF-kappaB signaling, 2009. Cardiovasc Res 84:119-126.

Xu J, Srinivas BP, Tay SY, Mak A, Yu X, Lee SG, Yang H, Govindarajan KR, Leong B, Bourque G, Mathavan S, and Roy S. Genomewide expression profiling in the zebrafish embryo identifies target genes regulated by Hedgehog signaling during vertebrate development, 2006. Genetics 174:735-752.

Yang L, Kemadjou JR, Zinsmeister C, Bauer M, Legradi J, Muller F, Pankratz M, Jakel J, and Strahle U. Transcriptional profiling reveals barcode-like toxicogenomic responses in the zebrafish embryo, 2007. Genome Biol 8:R227.

Yoshikawa K, Imai K, Seki T, Higashi-Kuwata N, Kojima N, Yuuda M, Koyasu K, Sone H, Sato M, Senoo H, and Irie T. Distribution of retinylester-storing stellate cells in the arrowtooth halibut, Atheresthes evermanni, 2006. Comp Biochem Physiol A Mol Integr Physiol 145:280-286.

Zelcer N, and Tontonoz P. Liver X receptors as integrators of metabolic and inflammatory signaling, 2006. J Clin Invest 116:607-614.

Zon LI, and Peterson RT. In vivo drug discovery in the zebrafish, 2005. Nat Rev Drug Discov 4:35-44.